ANNUAL REPORT TO ONR ON GROUP IV ALE PROJECT, OCTOBER, 1993

ONR Contract #N00014-91-C-0080

Submitted by

S. M. Gates, F. J. Himpsel, S. S. Iyer,
D. D. Koleske, D. Lapiano-Smith, F. R. McFeely,
F. Guarin, A. Powell and B. A. Scott

IBM Research Division
T. J. Watson Research Center
Yorktown Heights, New York

IBM

Table of Contents

		page
A.	Surface Species in ALE Identified by Photoelectron Spectroscopy	2
	References	3
	Figures	5
B.	Si ALE Process Development, and Atomic H Reactions	8
	References	11
	Figures	12
C.	Atomic Layer Epitaxy of Column IV Materials	18
	References	20
	Figures	21
	Appendix A	
	Appendix B	
	Appendix C	
	Appendix D	

A. Surface Species in ALE Identified by Photoelectron Spectroscopy

1. Motivation

The general goal of this work is to identify the chemical species that are present at the surface during atomic layer epitaxy (ALE). Particularly interesting is the nature of the passivation layer that terminates the broken bonds at the semiconductor surface in the first ALE step. Likewise, we follow the removal of the passivating species in the second step by thermal decomposition, desorption, irradiation, or chemical reaction. We use mainly surface-sensitive photoelectron spectroscopy at our beam line at the National Synchrotron Light Source (NSLS) in Brookhaven. During the past year we have built a new beam line at the Advanced Light Source (ALS) in Berkeley, which will exhibit 10^4 times higher brightness than NSLS. We expect the ALS beam line to become operational late '93 or early '94.

After identifying the chemical reactions at the surface we expect to be able to make suggestions for possible ALE processes, which then can be tested by other members of this project, who have the equipment to determine the growth rate and to produce device structures. This approach has already worked in one instance (Si ALE via SiH_2Cl_2 and atomic hydrogen), where an ALE process proposed from surface spectroscopy has been found to work by S. M. Gates.

2) Insulators on Si, Ge ('91, Refs. 1,2)

Our earliest efforts focussed on the epitaxial growth of insulating layers on Si and Ge with thickness control on an atomic scale. Such structures are interesting for three-dimensional device structures (e.g. stacked CMOS), and for the modification of band offsets (e.g. at an emitter-base junction). After extensive studies of the CaF_2/Si(111) interface (Ref. 2), which exhibits dramatic changes in the band gap and large band offsets at the interface, we found that high quality LiF could be grown on Ge(100) (Ref. 1). A particularly noteworthy feature of these LiF(100) films is their negative electron affinity, the largest found in ordinary solids. It causes a large spike of photoemitted electrons near the vacuum level (Fig. 1), similar to that previously observed for H-terminated diamond. The latter has attracted recent interest in the context of flat panel displays driven by electron emission from an array of tips.

3) Si on Si ('91, '92, Refs. 3-6)

Our starting point for investigating ALE of Si was the original process proposed by Nishizawa et al., i.e. alternating cycles of SiH_2Cl_2 and H_2. A naive model of this process would suggest that during the adsorption of SiH_2Cl_2 the weaker-bound H_2 desorbs, and the surface becomes saturated with $SiCl_2$ species. Using core level photoelectron spectroscopy (Ref. 3) we found that the surface is indeed Cl-passivated, but surprisingly by $SiCl_1$ species, not $SiCl_2$ (Fig. 2). This indicates dimerization of surface Si atoms, which reduces the density of broken bands by a factor of two, as on clean Si(100). Under ALE conditions (above 600°C) a full monolayer of Si atoms is found to bond to Cl on Si(100), using the area of the hatched $SiCl_1$ core level peak in Fig. 2. At room temperature only half a layer of Si is saturated by Cl, the other half presumably by H from

SiH_2Cl_2. On Si(111) we find less Cl-terminated Si surface atoms than on Si(100), which is explained by the lower broken bond density of Si(111).

Regarding the activation step of Si ALE we found that H_2 does not remove Cl from the surface (it was probably desorbed thermally in the work of Nishizawa et al.). Our proposal to use atomic H instead of molecular H_2 for removing the Cl passivation layer was successfully carried out by S. M. Gates.

SiC on Si ('93, Refs. 5,6)

Already in the course of our Si ALE work we tested C-containing compounds, such as diethylsilane. It was found that ethyl groups saturate the surface (Fig. 3, Ref. 5). Likewise, methyl groups saturate the surface when using dimethylsilane. These different alkyl species can be distinguished very nicely at the surface by the splitting of the C2s level, which directly gives the number of C atoms in the alkyl group. This new detection method for alkyl groups at surfaces might be quite useful in III-V and II-VI CVD and ALE, where these are common ligands.

In order to obtain criteria for the use of various compounds in SiC ALE we systematically varied the ligands. With alkyl ligands (diethlsilane and dimethylsilane) we found that not enough C was deposited since a large fraction of the alkyl groups desorbs upon heating instead of dehydrogenating. Only with a continuous flow of diethylsilane at 600-700°C did we find deposition of SiC. Replacing H by the more strongly-bound Cl (e.g. via trichloromethylsilane) cause the molecule to become so inert that a significant OH contamination of the Si surface occurred before completing a monolayer. From such scouting experiments we concluded that a useful compound for SiC ALE has to fulfill two criteria: a) It has to contain H ligands in order to facilitate sticking. b) The carbon has to be bound to two (or more) Si atoms in order to prevent it from desorbing during activation. A compound that fulfills these criteria (H_3Si-C-SiH_3) is under investigation.

References (Work supported by ONR)

1. D. A. Lapiano-Smith, E. A. Eklund, F. J. Himpsel, and L. J. Terminello, "Epitaxy of LiF on Ge(100)", Appl. Phys. Lett. **59**, 2174 (1991).
2. F. J. Himpsel, "Epitaxy of CaF_2/Si(111) and LiF/Ge(100)", invited talk at the WEH-Symposium on "Adsorption on Ordered Surfaces of Ionic Solids and Thin Films", Bad Honnef, Germany, Feb. 15-17, 1993; to appear in *Adsorption on ordered surfaces of ionic solids and thin films* ed. by H.-J. Freund and E. Umbach, Springer (Heidelberg).
3. J. A. Yarmoff, D. K. Shuh, T. D. Durbin, C. W. Lo, D. A. Lapiano-Smith, F. R. McFeely, and F. J. Himpsel, "Atomic Layer Epitaxy of Silicon by Dichlorosilane Studied with Core Level Spectroscopy", J. Vac. Sci. Technol. A **10**, 2303 (1992).
4. D.A. Lapiano-Smith and F. R. McFeely, "The Chemisorption and Reaction of GeCl4 with Si(100)", Thin Solid Films **225**, 187 (1993). The ONR acknowledgement was inadvertently omitted on this publication.
5. D. A. Lapiano-Smith, F. J. Himpsel, and L. J. Terminello, "The Chemisorption and Reaction of Diethylsilane on Silicon (100) and (111) Surfaces", J. Appl. Phys. **74**, Oct. 15 (1993).

6. D. A. Lapiano-Smith and F. J. Himpsel, "The Chemisorption and Reaction of Diethylsilane on Si(100) and (111) Surfaces Studied by Soft X-ray Photoemission", Proceedings of the MRS Spring 1993 Meeting, San Francisco, April 12-16, 1993.

Fig. 1 Band gap and negative electron affinity of LiF grown epitaxially on Ge(100) (from Ref. 2). The spike of high electron emission near the vacuum level (≈4eV) is characteristic of negative affinity surfaces.

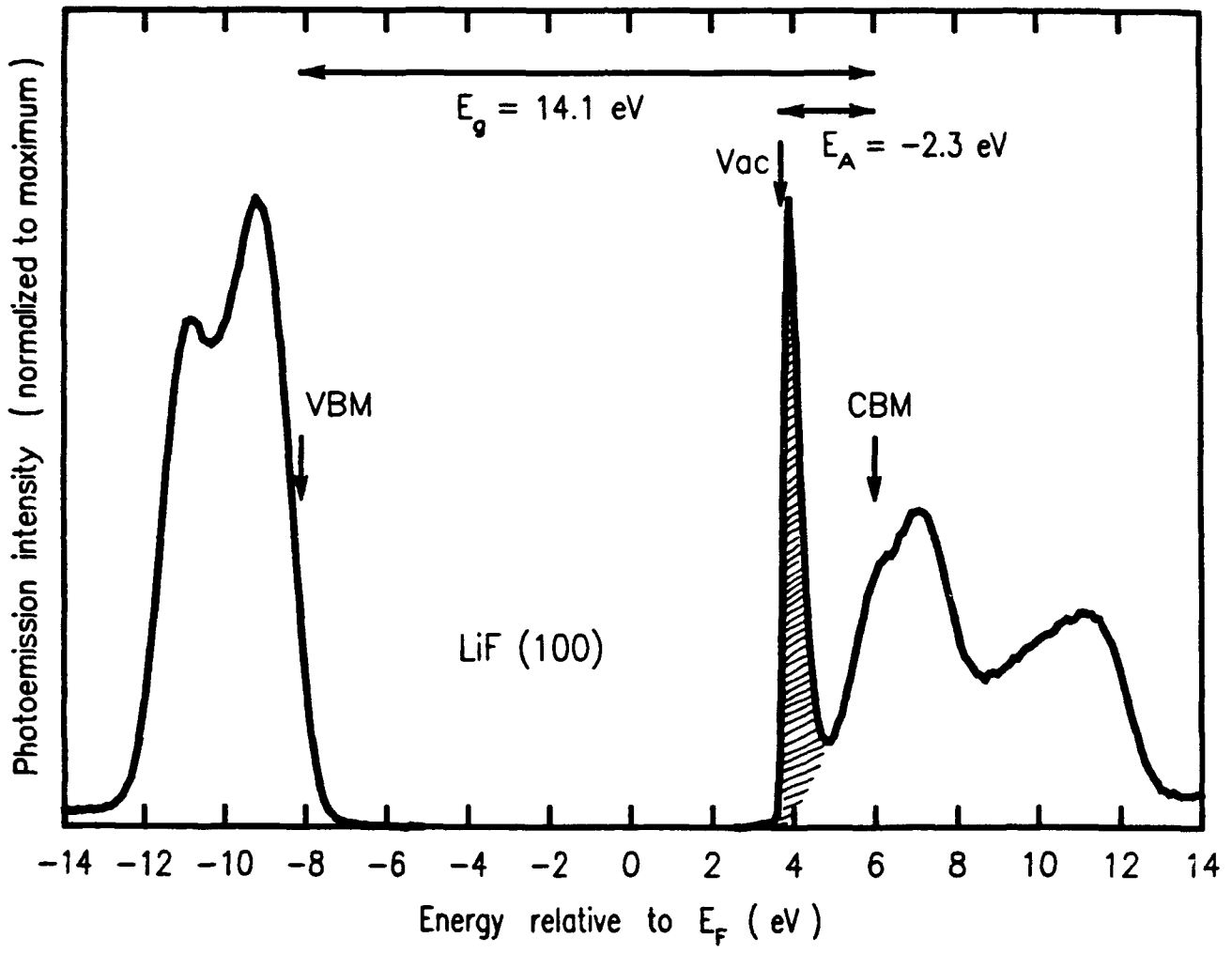

Fig. 2 Termination of the Si(100) by monochloride species after adsorption of SiH_2Cl_2 at 600°C (from Ref. 3).

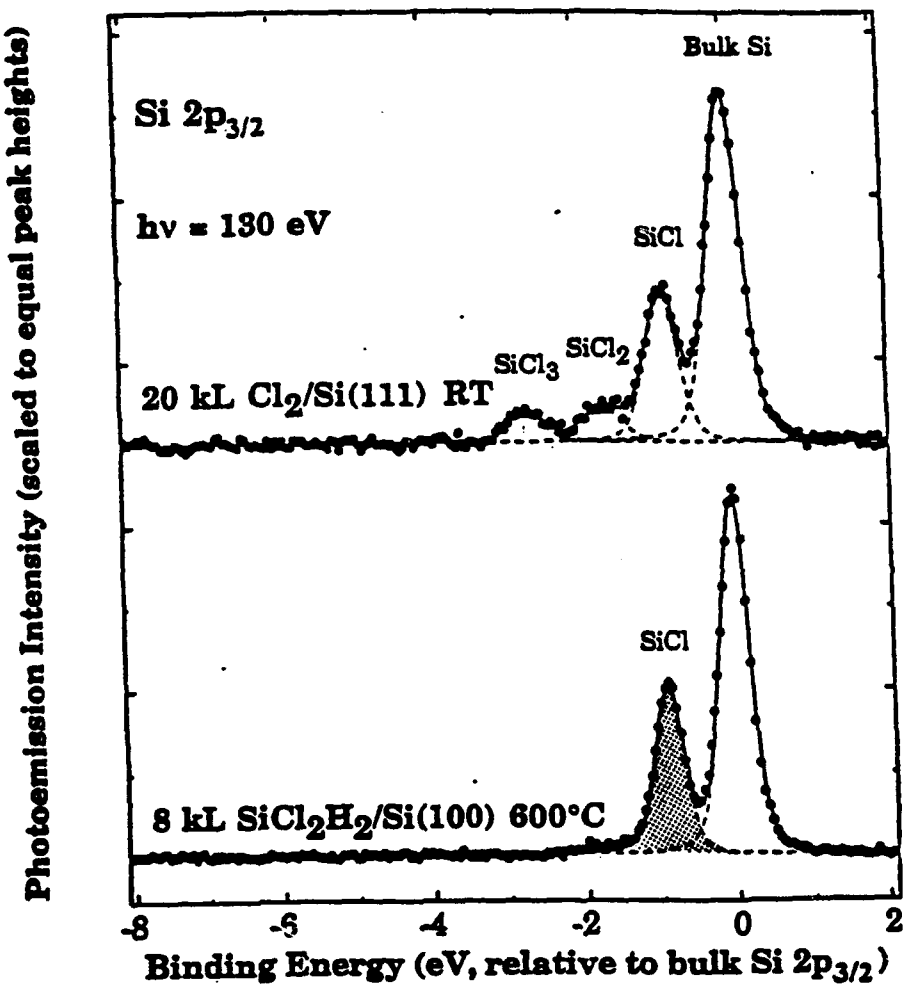

Fig. 3 Identification of ethyl and methyl groups at the Si(100) surface using the split C2s level. The number of C2s components gives directly the number of the C atoms in the alkyl group.

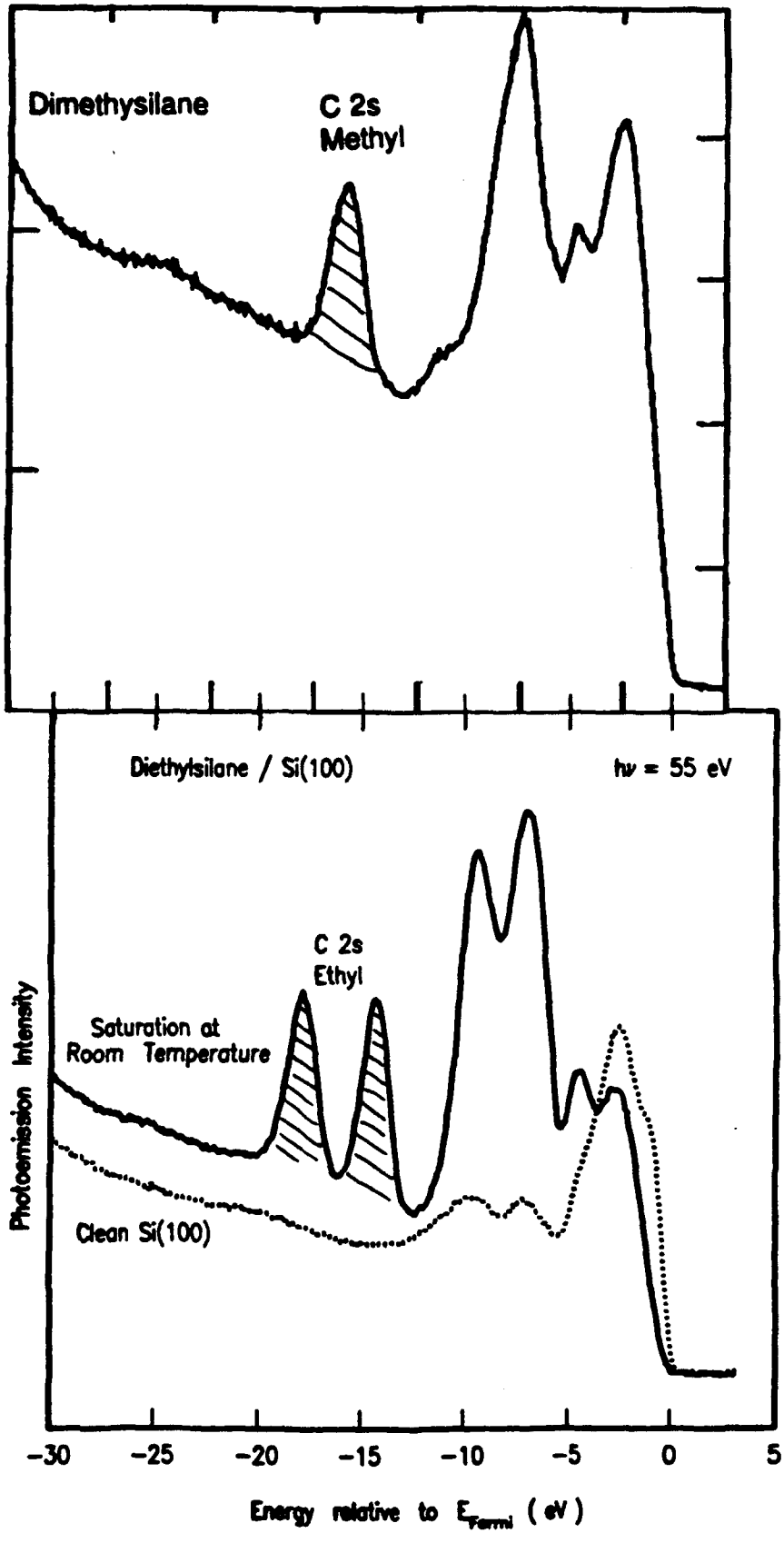

B. Si ALE Process Development, and Atomic H Reactions

Our work on Si ALE Processes is described in 4 Parts, listed below. Reference is made to 2 papers submitted for publication, which are attached as Appendices A & B.

1. Summary of the Si_2Cl_6 + Si_2H_6 process for Si ALE.
   This work was reported in the Oct. '92 Progress Report.
2. Summary of the Atomic H + $SiCl_2H_2$ and the Atomic H + Si_2Cl_6 processes for Si ALE.
3. Summary of work on Nitrogen as an elemental marker of the initial Si surface, as a tool for the study of Si ALE.
4. Status of research on H self-abstraction by H_{at} on C, Si and Ge.

1. Summary of the Si_2Cl_6 + Si_2H_6 Process.

An isothermal process for Si ALE using alternating pulses of Si_2Cl_6 + Si_2H_6 has been described in APL **62** (1993) 510. This process features isothermal Si epitaxy, with ± 2 ML thickness control, and abrupt Si/Ge(100) heterointerfaces. The key attributes of this process are as follows.

- Only stable, commercially available molecules are used.
- Isothermal, ≃475 ±15 °C.
- Thickness Control To ±2 ML,
  Proportional To # Cycles.
- Abrupt Si/Ge(100) Heterointerfaces.
  No Detectable Ge Out-Diffusion.
- Practical, Scalable To Large Substrates.
- Hexachlorodisilane Dose Is Self-Limiting.
  Disilane Dose Is Not Self-Limiting.
- ΔH Positive, ΔS Large & Positive. (see S.M. Gates, J. Phys. Chem. **96** (1992) 10439).

2. Summary of the H_{at} Based Processes.

Isothermal processes for Si ALE using alternating pulses of H_{at} and a chlorosilane (either $SiCl_2H_2$ or Si_2Cl_6) have been investigated. These provide isothermal Si deposition, with amount of deposited Si proportional to number of ALE cycles. Non-abrupt Si/Ge(100) heterointerfaces are formed due to the "chemical heating" or "chemical annealing" effects of H_{at}, which are discussed below. The Atomic H + Si_2Cl_6 process is described in detail in Appendix A. The Atomic H + $SiCl_2H_2$ process is discussed below. Key findings regarding H_{at} + chlorosilane ALE are as follows.

- Alternating pulses of Si_2Cl_6 + H_{at}, or of $SiCl_2H_2$ + H_{at}, are used. The chlorosilanes are commercially available.
- Isothermal, ≃525 ± 25 °C.
- Deposited Si is < 1 ML/Cycle, but is proportional to number of ALE cycles.
- A non-Abrupt Si/Ge(100) heterointerface, i.e. a mixed Si/Ge alloy, is formed on Ge(100).

- Anticipated problems with H_{at} are uniform flux over large areas, chemical annealing (see below) and etching as SiH_x species (see S.M. Gates, et al., Surface Science **207** (1989) 364).
- Self-Limiting In Si Deposition,
  H_{at} Effects Are Dose Dependant.
- ΔH Negative, $\Delta S \simeq 0$
  Thermodynamics Fit Pattern Of ALE Reaction,
  Based On ZnS, GaAs, Metal Oxides (see S.M. Gates, J. Phys. Chem. **96** (1992) 10439).

The morphology of deposited Si on Ge(100) surfaces was studied using Direct Recoiling (DR) methods. By scanning the incident angle of the alkali ion beam with respect to the surface plane, α, growth morphology is conveniently examined *in situ*. Figure 4 and Figure 5 have the same format. Time-of-flight (TOF) DR spectra appear in the bottom panel for 3 different α values, and the trends are plotted in the top panel as a function of α. Figure 4 is from one cycle of the Si_2Cl_6 + Si_2H_6 process at 465°C, producing an abrupt heterolayer ($\simeq$ 5 ML thick) of Si on Ge(100). The Ge DR signal is zero at small α, and rises to a barely detectable signal only for $\alpha > 20°$. This is our standard for a buried Ge surface. Figure 5 is from 2 and 4 cycles of the Atomic H + $SiCl_2H_2$ process at 465°C, producing a mixed Si/Ge alloy layer of Si deposited on Ge(100). The Ge DR signal is large at all α values, with a relatively constant signal as a function of α.

The data of Figure 5 prove that Si is deposited by this process. In Appendix A, a very similar process is shown to be self-limiting in the Si deposition step. The Si on Ge(100) layer (Figure 4), and the mixed Si/Ge alloy (Figure 5) both exhibit RHEED patterns proving epitaxial growth (see D. D. Koleske and S. M. Gates, to be submitted to J. Appl. Phys.).

3. Nitrogen Marking of Initial Si(100) Interfaces.

In the Journal of Applied Physics (see D.D. Koleske and S.M. Gates, JAP **74** (1993) 4245), we have reported the use of nitrogen (N) as an elemental marker in the study of Si ALE. A saturation coverage of NH_3 on Si(100) at room temperature results in a sub-monolayer N coverage of $\simeq$ 1/3-1/2 ML after heating to 600°C to remove the hydrogen. After this anneal, the N resides in sub-surface sites, probably between the 1st and 2nd layers of Si. Figure 6 shows TOF Direct Recoiling incident angle (α) scans, similar to the top panel of Figures 4 and 5, but using the Si(100) surface marked with N. Scans of α for the N marked surface (curve A) and this surface after 1 (curve C) and 2 (curve E) complete cycles of the Si_2Cl_6 + Si_2H_6 ALE process (see above) appear in Figure 6. As Si is deposited by running the Si_2Cl_6 + Si_2H_6 ALE process for 1 and then 2 cycles, the DR N intensity at each α decreases. Reflection High Energy Electron Diffraction confirmed that this Si is epitaxial. These results demonstrate that N is a useful "marker element" for the study of Si on Si homoepitaxy by ALE. At 600°C and below, N does not diffuse on a timescale of 10-30 minutes, and $\simeq$ 1/3-1/2 ML coverage of N does not inhibit the epitaxial growth of Si. Previously, the marker elements boron, germanium and tin were all found unsatisfactory. These 3 elements all migrate (diffuse) at growth temperatures of $\simeq$ 400-500°C (see S.M. Gates and D.D. Koleske, Appl. Phys. Lett. **61** (1992) 309).

4. Self-Abstraction of Chemisorbed H by H_{at}

Reactions (1) and (2) provide a mechanism for "chemical annealing" or "chemical heating" of a Si surface exposed to H_{at}. Surface dangling bonds are denoted by _-Si. (While "heating" is an acceptable term, "temperature" is not, because this is a non-equilibrium effect.)

$$H_{at} + \_ - Si \rightarrow H - Si \quad (1)$$

$$H_{at} + D - Si \rightarrow HD(g) + \_ - Si. \quad (2)$$

The abstraction of chemisorbed H (or D) by H_{at} incident from the gas phase *creating dangling bonds* is reaction (2). Reaction (1) delivers the full Si-H bond energy, about 3 eV ($\simeq$ 80 Kcal/mole) to the surface. The sum of (1) and (2) is reaction (3), the surface catalyzed recombination of H and D.

$$2 + H_{at} + D_{at} \rightarrow HD(g) \quad (3)$$

This effect is known in diamond CVD {1}, and several papers on "chemical annealing" of amorphous Si using H_{at} have appeared from a group at Tokyo Institute of Technology {2}.

We are investigating the abstraction of chemisorbed H (or D) by D_{at} (or H_{at}) on Ge, Si, and diamond surfaces. SiC is intended for future work. Appendix B is a copy of a paper from the Oct. 1, 1993, Journal of Chemical Physics, for the specific case of H_{at} → D-Si(100). Figure 7 shows the experimental arrangement. Figure 8 shows TOF spectra of recoiled H^+ and D^+ ions taken at various times (starting with a D saturated surface) of H_{at} exposure. A full experiment contains many TOF spectra at various reaction times, and a plot confirming the kinetics are 1st order is shown as Figure 9. The slope of the solid line in Figure 9 gives the rate constant for reaction (2), under the assumption that reaction (1) is faster than reaction (2).

We have compared the rates of reaction (2) with H_{at} → D-Si and with D_{at} → H-Si on both Si(100), Si(111) and Ge(100), and all these systems exhibit 1st order kinetics. Dr. Bret Jackson of The University of Massachussetts is collaborating by providing time-dependant quantum mechanical calculations, similar to his calculations for the same reactions on copper and tungsten surfaces {3}.

It is noteworthy that reaction (2), abstraction, is very rapid. For the H_{at} → D-Si case, the rate is 0.36 times the rate of (1). Preliminary results on the D_{at} → H-Si case indicate the rate is roughly the same. The activation energies are consistently 1 $\pm$ 0.5 Kcal/mole, close to zero. These rate measurements for reaction (2) provide crucial input for models of heat delivery to the Si surface in a flux of H_{at}. Similar studies for polycrystalline diamond surfaces are in progress, in collaboration with J. Butler's group at NRL.

References

1. W.A. Yarbrough, K. Tankala, M. Mecray, and T. DebRoy; Appl. Phys. Lett. **60**, 2068 (1992).
2. H. Shirai, D. Das, J.-I. Hanna, and I. Shimizu; Appl. Phys. Lett. **59**, 1096 (1991).
   I. Shimuzu; J. Non-Cryst. Solids **114**, 145 (1989).
   H. Shirai, J.-I. Hanna, I. Shimizu; Jpn. J. Appl. Phys. **30**, L679 (1991).
3. B. Jackson and M. Persson; J. Chem. Phys. **96**, 2378 (1992).

S.M. Gates & D.D. Koleske, Publications Supported by ONR on Si ALE, October 1991 - October 1993.

1. S.M. Gates and D.D. Koleske, "Elemental Marking of Si on Si(100) Interfaces" Appl. Phys. Lett., **61**, 309 (1992).
2. D.D. Koleske, S.M. Gates and D.B. Beach, "Growth Of Si On Si(100) Via H/Cl Exchange, And The Effect Of Interfacial Boron", J. Appl. Phys. **72**, 4073 (1992).
3. D.D. Koleske, S.M. Gates and D.B. Beach, "Precursors For Si Atomic Layer Epitaxy: Real Time Adsorption Studies on Si(100)", Appl. Phys. Lett. **61**, 1802 (1992).
4. S.M. Gates, "Comparison Of Chemical Schemes For Si Atomic Layer Epitaxy", J. Phys. Chem. **96**, 10439 (1992).
5. S.M. Gates, D.D. Koleske, J.R. Heath and M. Copel, "Epitaxial Si Films On Ge(100) Grown Via H/Cl Exchange", Appl. Phys. Lett **62**, 510 (1993).
6. D.D. Koleske and S.M. Gates, "Influence of Si Surface Structure On Reaction Mechanism: Atomic Hydrogen + Adsorbed Br", J. Chem. Phys., Communications **98**, 5091 (1993).
7. D.D. Koleske and S.M. Gates, "Surface Morphology Of Si On Si(100) Grown Below 500°C Using H/Cl Exchange Chemistry", J. Appl. Phys. **74**, 4245 (1993).
8. D.D. Koleske and S.M. Gates, "Kinetics of Atomic Hydrogen + Adsorbed Br Reactions on Si(100) and Si(111) Surfaces", J. Chem. Phys., in press for 11/93.
9. D. D. Koleske, S. M. Gates and J. A. Schultz, "Facile Abstraction of Chemisorbed D on Si(100) by Atomic H", J. Chem. Phys., Communications, **99**, 5619 (1993).
10. D.D. Koleske and S.M. Gates, "Atomic Layer Epitaxy Of Si On Ge(100) Using Si_2Cl_6 And Atomic Hydrogen", Appl. Phys. Lett., submitted.
11. S.M. Gates and D.D. Koleske, "Dopants On Si(100) Surfaces: Useful Probes Of Si Atomic Layer Epitaxy?", Thin Solid Films **225**, 160 (1993).
12. D.D. Koleske, S.M. Gates and D.B. Beach, "Potential Si ALE Processes Using Halogenated Si Precursors" Thin Solid Films **225**, 173 (1993).

Fig. 4 Incident angle, α scan, of the elemental signal vs. α for $\simeq$ 3 ML of Si (which is H terminated) grown using alternating cycles of Si_2H_6 and Si_2Cl_6 on Ge(100) at 465°C. The top panel shows the trends in elemental signal intensity from the time-of-flight direct recoil (DR) spectra, normalized to the maximum DR signal. In an α scan, surface elements (H, for example) have maximum DR intensity at small α, while bulk elements (Ge, for example) have maximum DR signal at large α. Note that Ge and to a lessor degree Si behave as bulk elements, with Ge having a vanishingly small DR signal even at high α (see bottom panel).

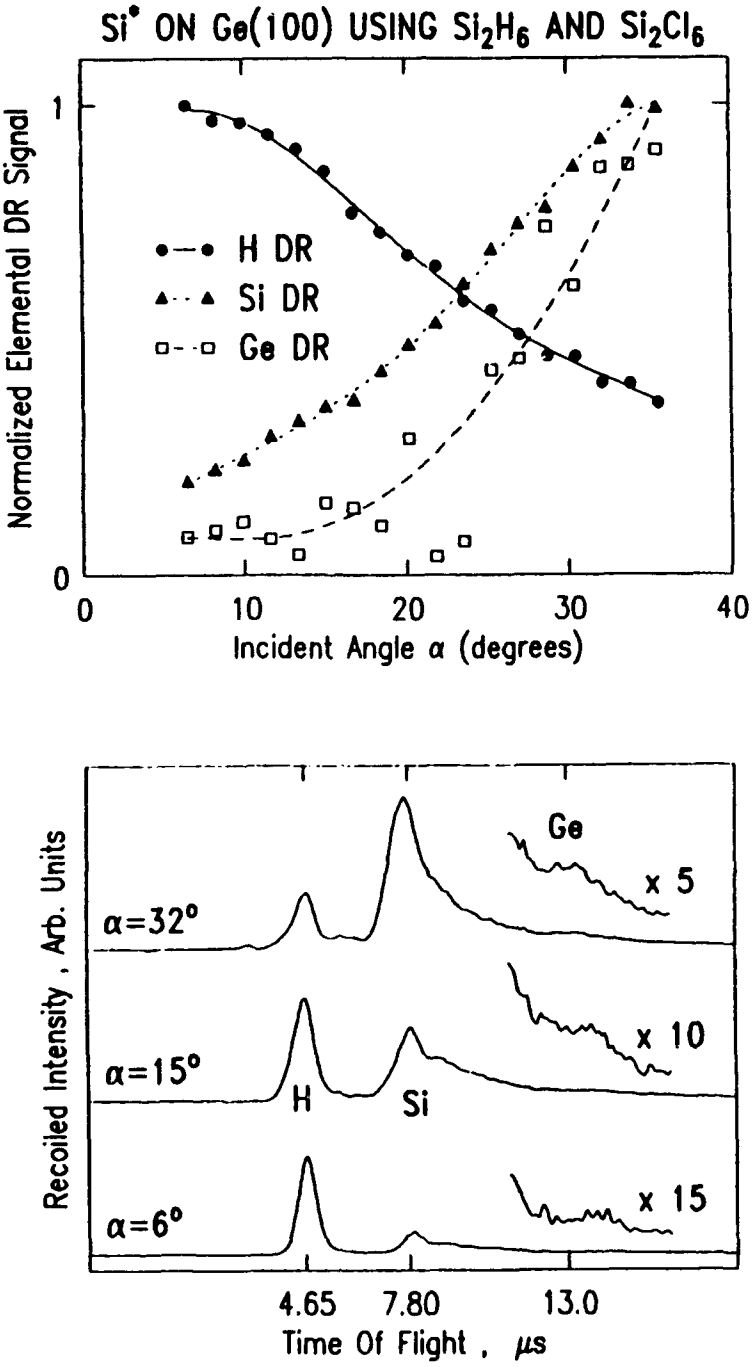

Fig. 5 Incident angle, α scan, exactly as Figure 4, except the Si is grown using alternating cycles of $SiCl_2H_2$ and H_{at} (on Ge(100 at 465°C). This data proves that Si is deposited using this H_{at} based process for Si ALE. The top panel shows α scans of the Ge_{DR} signal for 2 and 4 growth cycles. The Si_{DR} α scan after 2 cycles looks the same as the Si_{DR} α scan after 4 cycles and therefore is not shown.

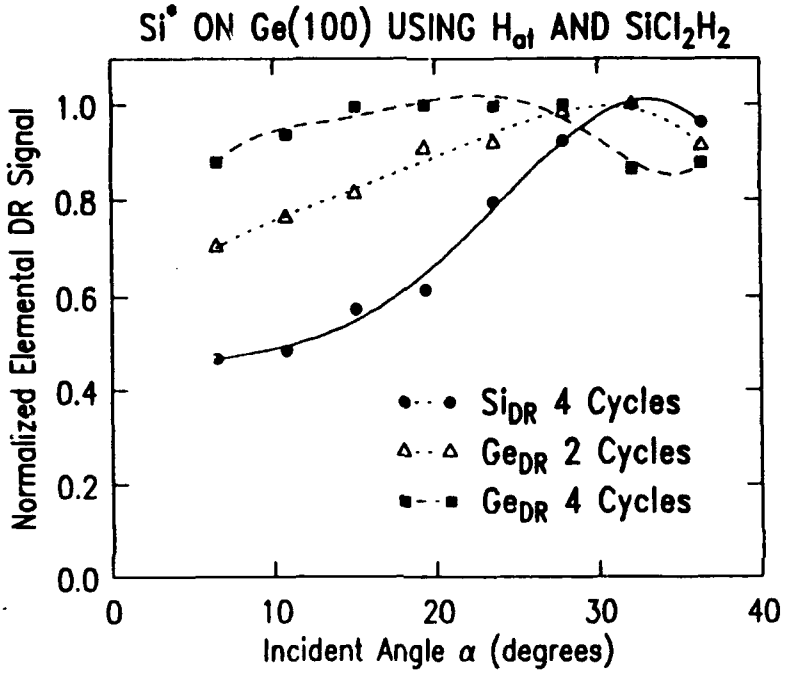

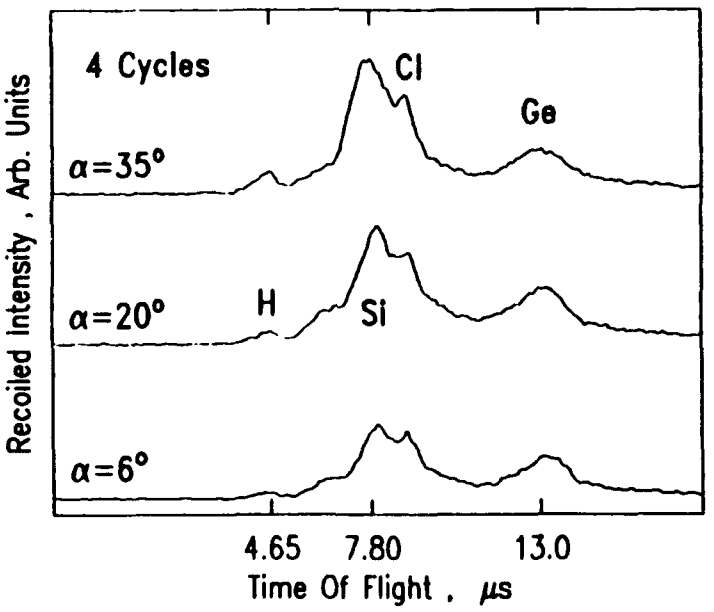

Fig. 6 Incident angle, α scan, of the elemental DR signal vs. α for growth of Si on the nitrogen marked Si(100) surface, which is designated N/Si(100). Attenuation of the N signal proves that Si is deposited. Only the N_{DR} intensity is plotted vs. α for N/Si(100) (curve A) and Cl terminated surfaces (curves C and E). The inset shows the H_{DR}, N_{DR}, and Si_{DR} intensities vs. α for ammonia deposited on clean Si(100) at $T_s = 100°C$. This surface is heated to 600°C to produce the N/Si(100) surface.

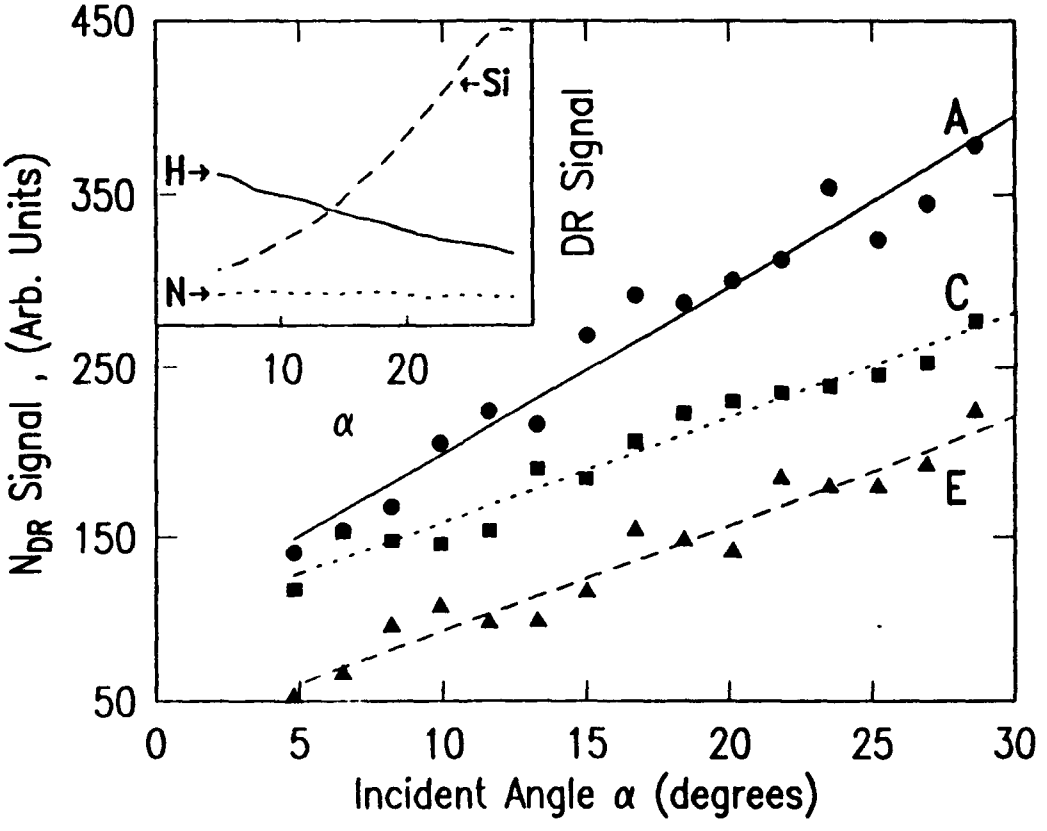

Fig. 7 Schematic diagram of low energy (4-10 keV) ion scattering and direct recoiling apparatus with reflectron time-of-flight analyzer. The incident Na^+ beam is 3° from the surface plane (α = 3 degrees), and the beam is pulsed at 50 kHz. The recoiled ions are detected at a recoil angle, $\Phi = 60°$, from the incident Na^+ beam. H_{at} and D_{at} are generated by flowing H_2 or D_2 through the chamber, and dissociating the gas on a resistively heated W filament at 1800 K.

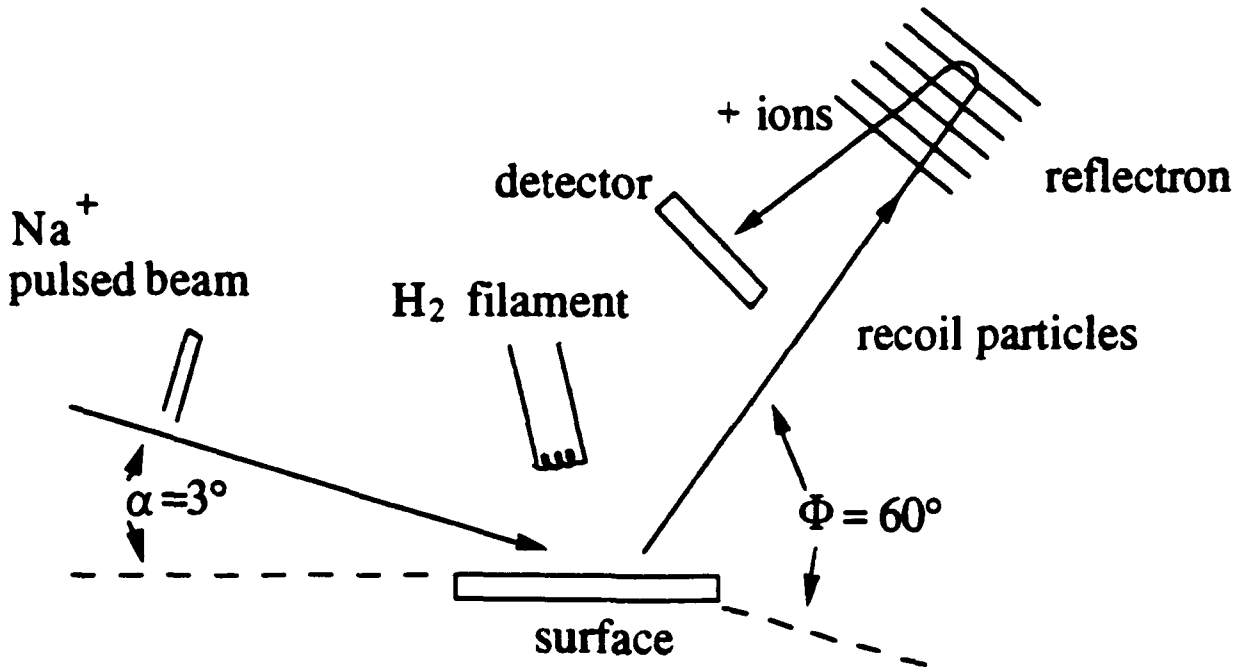

Fig. 8 A series of time-of-flight recoiled ion spectra showing H_{at} abstraction of D on Si(100) at 200°C. A: 1 monolayer (ML) of D on Si(100). B-D: this surface after 360, 720 and 1080 s of H_{at} exposure. E: 1 ML of H on Si(100)

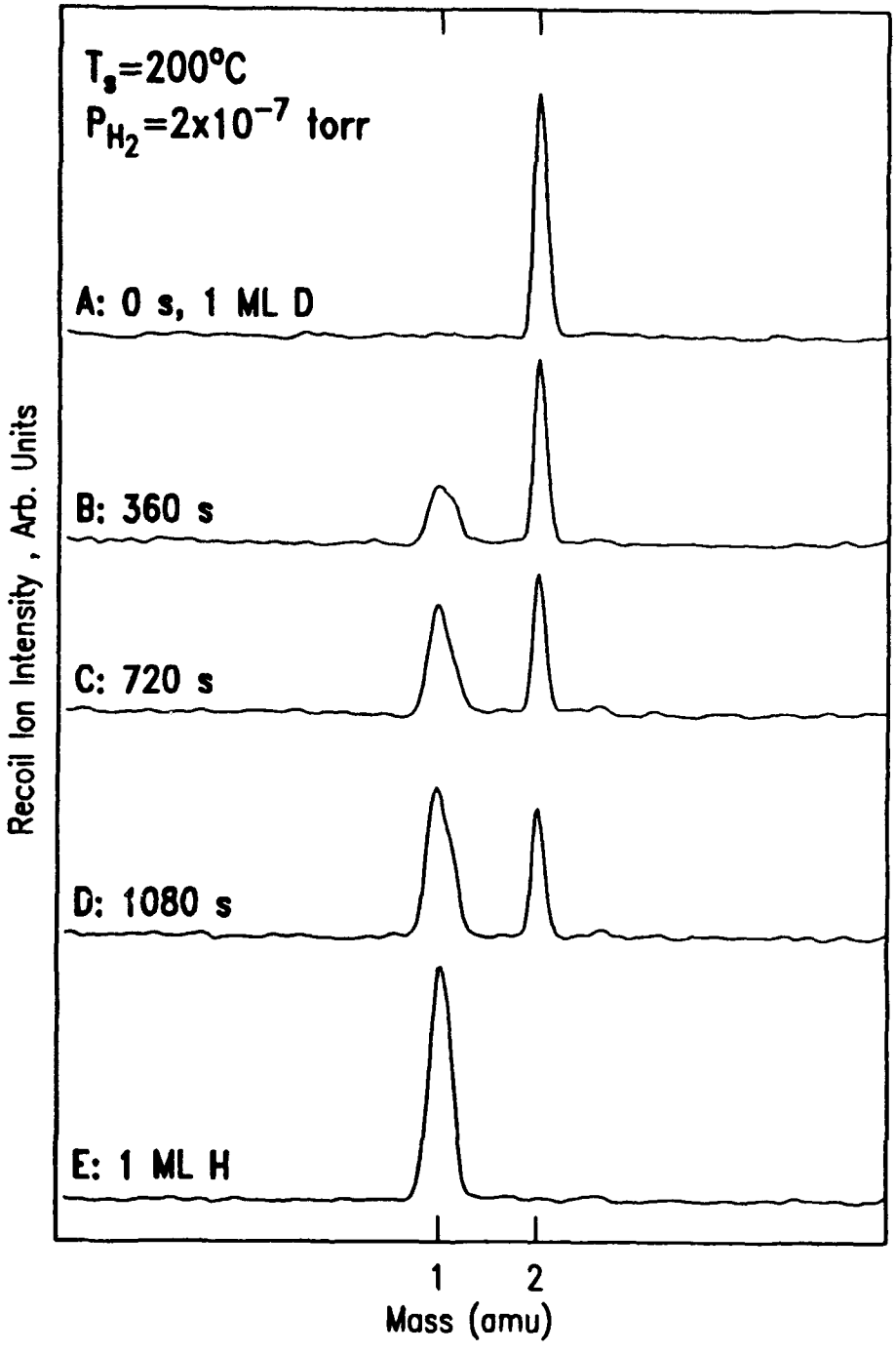

Fig. 9 Kinetic order plots for H_{at} abstraction of D on Si(100), with a pseudo-first order rate law plotted using solid dots (left ordinate) and a pseudo-second order rate law plotted using open squares (right ordinate). The solid line is a fit to the 1st order rate law (solid dots).

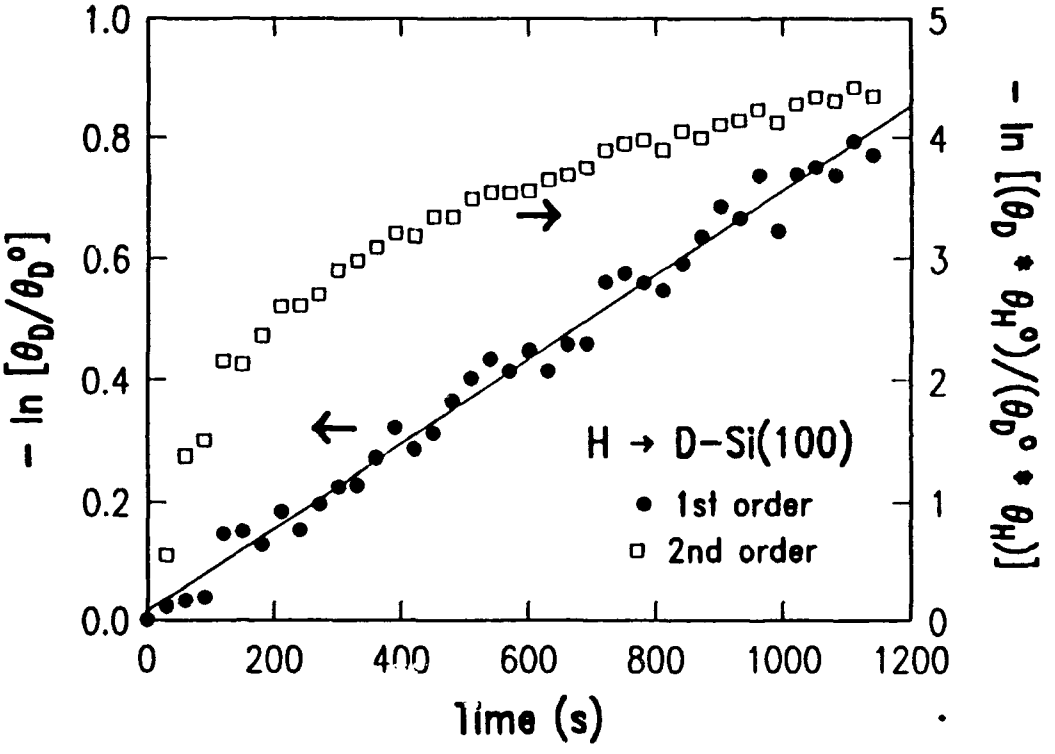

Atomic Layer Epitaxy of column IV materials

This section reports on progress made in three areas. These are

- Atomic Layer Doping of Si
- The growth of $Si_{1-y}C_y$ random alloys using a gas source C_2H_2 for C
- the growth of silicon carbide using gas sources with the potential for ALE

Atomic Layer Doping

Atomic Layer Doping promises an immediate application for self limiting surface reactions to introduce a known and controllable amount of electrically active dopant into a semiconductor layer either after or during growth. We have investigated the applicability of common n- and p-type dopants using either elemental or common precursor sources for this type of doping. Some findings have been reported earlier and are contained in Appendix C. We have since determined that elemental Sb does in fact offer the possibility of true atomic layer doping where a fraction of a monolayer (about 0.5) can be controllably and reproducibly deposited on an atomically clean surface. This method can be used in conjunction with solid source MBE or even as a diffusion source. Studies using B_2H_6 and AsH_3 have not been as successful. While B_2H_6 can be made adsorb on a clean surface at sufficiently low temperatures, the B thus incorporated was found to be inactive electrically presumably because it is well bonded to hydrogen. AsH_3 was not self limiting.

Silicon Carbon Alloys using acetylene as a carbon source

$Si_{1-y}C_y$ alloys have the potential for more versatile bandgap engineering. They permit the integration of layers with tensile strain directly on a bulk Si substrate. Additonally, when combined with the $Si_{1-x}Ge_x$ system, they allow for a more judicious tailoring of strain including the use of strain compensated layers. Until recently, the limited temperature window permitted the use of solid C sources only. More recently, as a result of our attempt to use atomic layer epitaxy methods for C incorporation we have determined that acetylene can be used as a source for $Si_{1-y}C_y$ alloys with a wider process window than is possible with solid sources. The details of these developements are contained in Appendix D.

Heteroepitaxial growth of β-SiC on Silicon substrates by solid and gas source MBE

A prime motivation for the ALE growth of Silicon Carbide is the potential of self limiting surface reactions to inhibit polymorphic instability. We hope that the use of ALE can sustain the growth of a monomorphic phase of silicon carbide, eg. β-SiC on say Si (100). Such a system would have tremendous utility for commercial applications, mainly because of large wafer sizes and lower cost. We need to however address the issue of the growth of thin film silicon carbide directly on Si (100) first to understand the process window that exists at present. In the previous section we discussed one limit viz., the production of alloys from both elemental and gas sources. In this section we describe the other limit of producing β-SiC films especially and study the differences between solid and gas sources of carbon in the deposition of β-SiC. We have conducted various MBE runs to grow βSiC layers via gas and solid source methods. For the gas source acetylene (C_2H_2) was utilized, while graphite was employed for the solid source growth. The MBE

approach for the ALE deposition of SiC allows us to take advantage of the in-situ diagnostic equipment available in the MBE chamber, and ability to combine both gas and solid source for the C permits more process latitude.

To grow good quality epitaxial β-SiC silicon substrates it is necessary to grow an intermediate buffer layer as initially reported by Nishino (1) and several other groups thereafter, either by utilizing CVD or Gas Source MBE approaches - good summaries of the many references can be found in overview articles by Davis et al (2,3,4) and Ivanov et al (5). One of the major stumbling blocks for the production of SiC on Si is the material quality of these intermediate layers where the defect levels are of the order of 10^{10}. It is in this area that we have initiated our research. We are investigating the formation of this intermediate layer using MBE with solid sources of both Si and C thus providing a wider selection of process parameters as well as an improvement in the defect density of the intermediate layer and hence in the epitaxially grown SiC. The first approach that we have tried for the production of this intermediate layer of Silicon Carbide on 125 mm. silicon substrates has provided encouraging preliminary results. This was done with a solid source MBE (described by Eberl et al (6)) with an elemental graphite filament that is resistively heated to sublimation temperature, i.e. above 3000 K. thus providing a pure elemental C beam containing no hydro- or halo-carbon sources. Amorphous carbon layers of different thickness ranging form 20 to 200 Angstroms were deposited from the solid source on Si (100) substrates, with no intentional heating of the wafers, the substrate temperature was about 150°C. due to the heat generated by the graphite source. After the initial layer deposition the wafers were then subjected to the anneal cycle shown in figure 10. XPS results before and after the anneal are presented in figure 11. A TEM Photograph for the sample that was deposited with 25 Angstroms of amorphous C and subjected to the anneal cycle just described is shown in figure 12, where the transformation to an epitaxial layer can be observed. Additional characterization of the diffraction patterns obtained on a planar TEM for a sample with a 67 Angstrom layer grown by this technique yielded a lattice parameter of 4.36 Angstroms, which clearly indicates the presence of a βSiC layer.

The temperature program for gas source growth of βSi-C on Si (111) substrates is shown in figure 13. Acetylene was introduced at 400°C. A one hour carbonization was performed at 970°C. the temperature was then lowered to 900°C. and the shutter opened for the silicon solid source, while maintaining the C_2H_2 pressure at $2X10^{-6}$ Torr, a layer of 1500 Angstroms was grown at a rate of 150 nm/min. The results of this growth were evaluated using XPS and X-Ray Diffraction (XRD). These are presented in figure 14. The XRD peak is in good agreement with the 35.6 deg. reported by Kim et al (7) for β-SiC on (111) Si.

We have obtained βSiC films both via gas and solid source approaches and are now concentrating on the optimization of parameters for a combined solid/gas C source approach tailored for the ALE deposition of very high quality βSiC layers. This should help us in understanding how the use of a self limiting ALE reaction may help in the stabilization of polytypes other than βSiC during growth.

References

1. S. Nishino, Y. Hazuki, H. Matsunami and T. Tanaka, "Chemical vapor deposition of single crystalline Beta-SiC films on Si substrates with sputtered SiC intermediate layer," J. Elechtrochem. Soc., **127** 2674 (1980).
2. R. Davis, G. Kelner, M. Shur, J. Palmour and J.Edmond, "Thin film deposition and microelectronic and optoelectronic device fabrication and characterization in monocrystalline alpha and beta Silicon Carbide," Proc. IEEE, **79** 677 (1991).
3. R. Davis, J. Palmour and J.Edmond, "Epitaxial thin film growth and device developments in monocrystalline Alpha and Beta SiC," Mat. Res. Soc. Symp. Proc. **162**, 463 (1990).
4. R. Davis, "Diamond and SiC thin films: present status and potential as wide band gap semiconducting material," Int. Journal of Materials and Product Technology, **4**, 81 (1989).
5. P. Ivanov and V Chelnokov, "Recent developments in SiC Single crystal electronics," Semicond. Sci. Technol. **7**, 863 (1992).
6. K. Eberl, S. Iyer, J. Tsang, M. Goorski, and F. LeGoues, J. Vac. Sci. Technol. B **10** 934 (1992).
7. K. Kim, S. Choi, K. Wang, "Growth of βSiC film on Si substrate using hydrocarbon gas and Si molecular beams in ultrahigh vacuum" J. Vac. Sci. Technol. B **10(2)**, 930 (1992).

Fig. 10 Thermal anneal cycle for conversion of amorphous C layer to β-SiC.

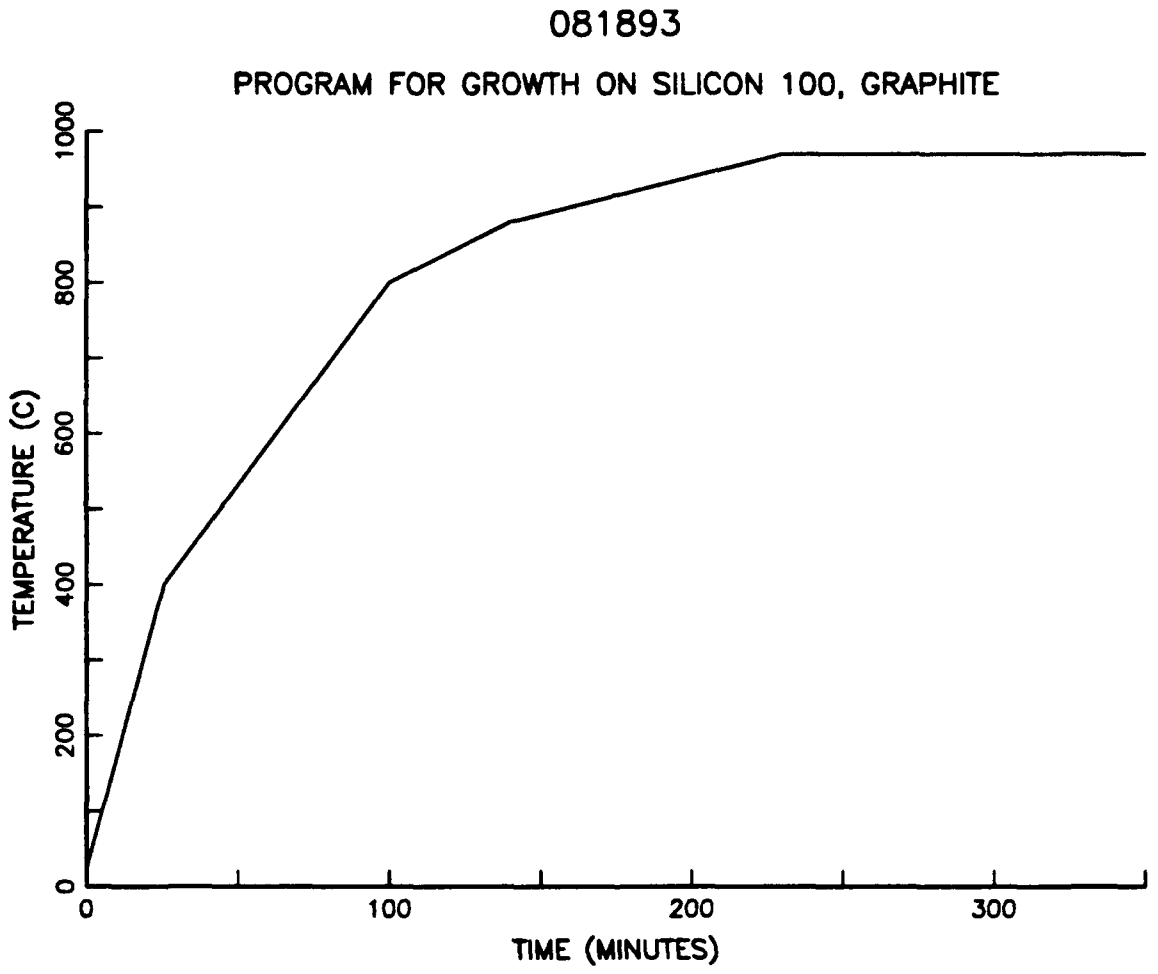

Fig. 11 XPS spectra before and after anneal. The shift in the C peak from 284 ev to 281 eV indicates that the material has changed phase to β-SiC

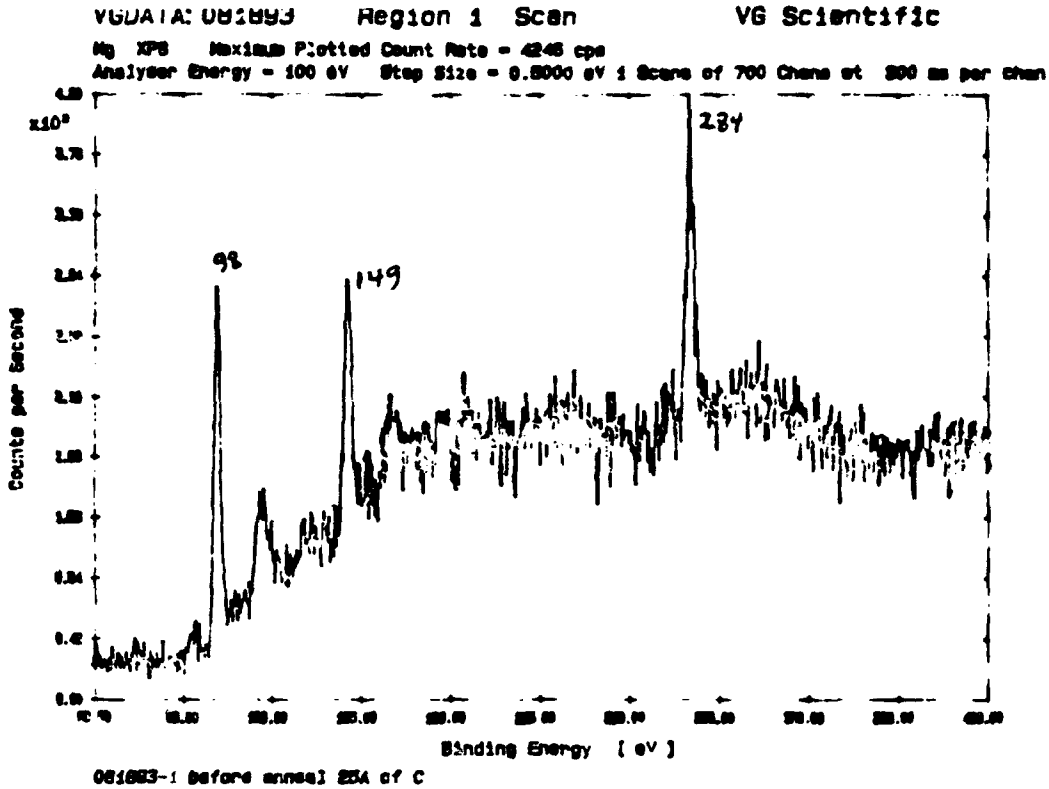

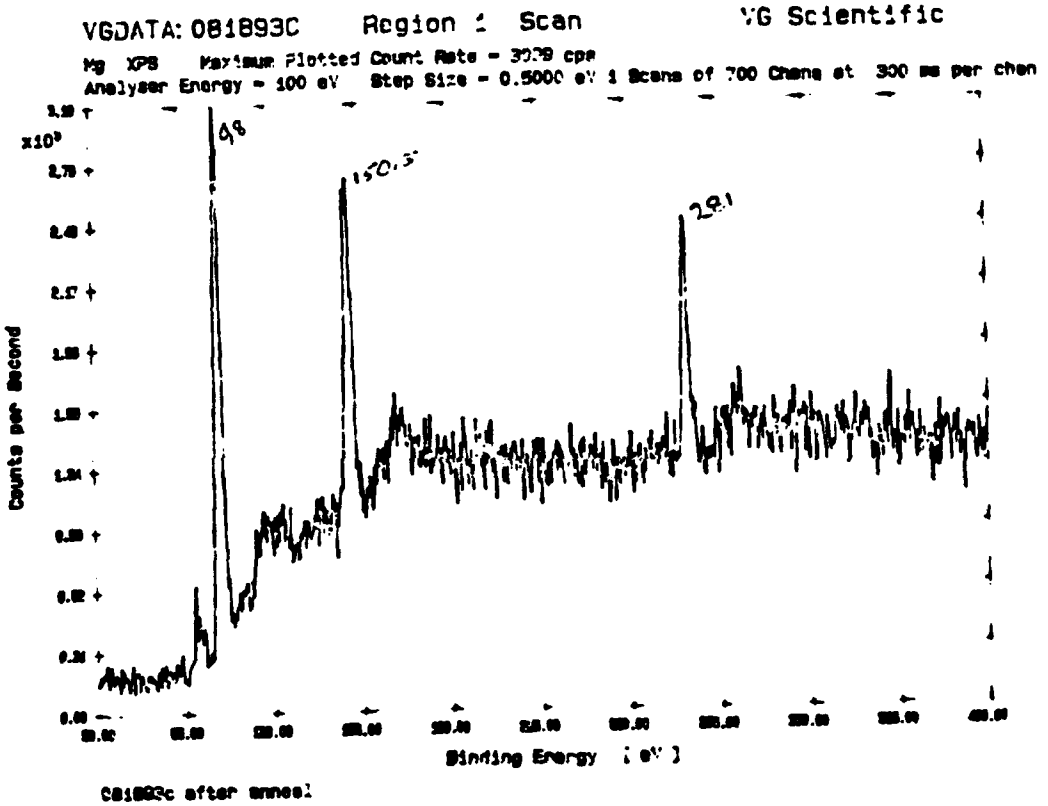

Fig 12 Cross sectional TEM of a post anneal sample with an original C thickness of 2.5 nm. The thin (5nm)epitaxial β-SiC layer can be seen on top of the Si substrate.

Fig. 13 Temperature program for growth of βSiC on Si(111) using C_2H_2 gas source and a solid Si source.

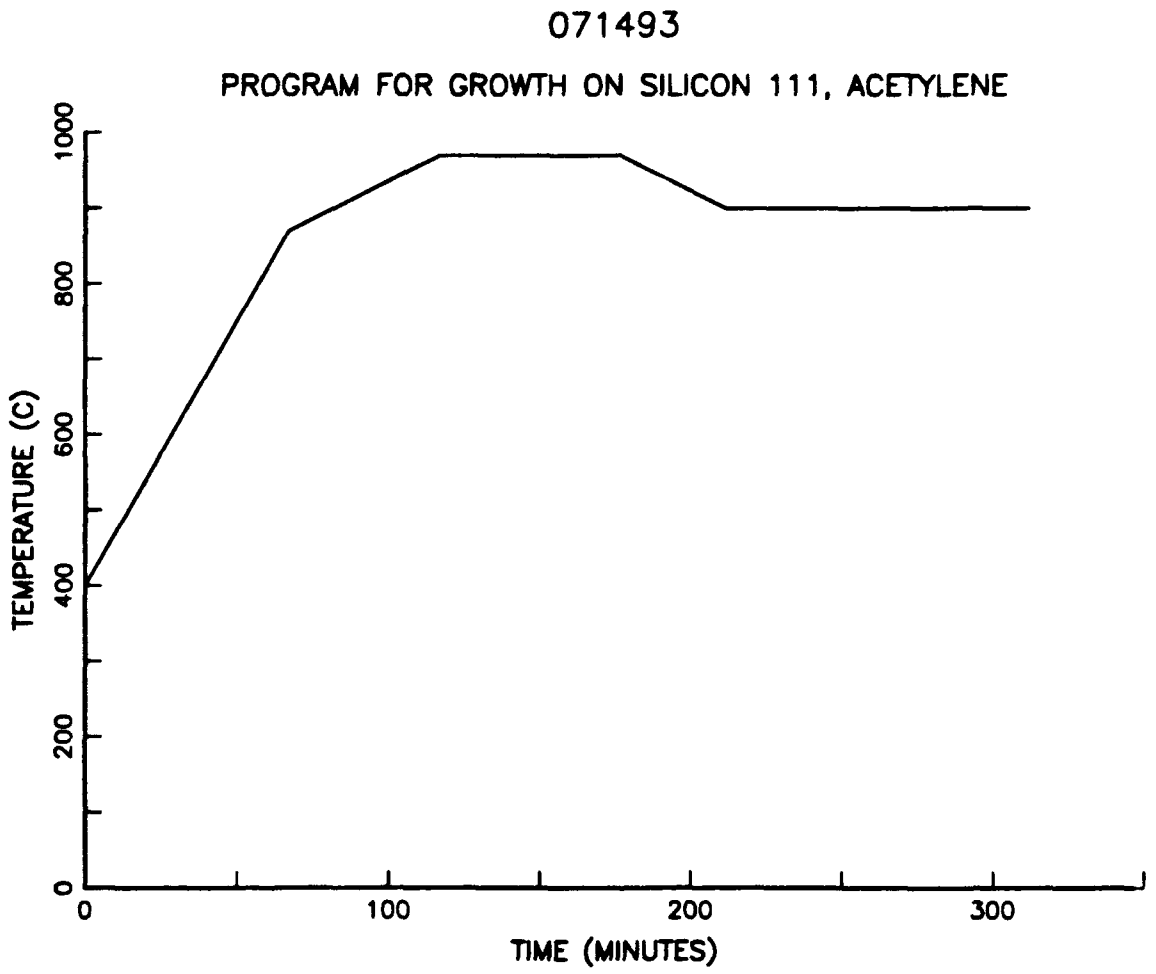

Fig. 14 XRD measurement for β-SiC/Si(111). Carbonization at 970°C for 60 min. (using C_2H_2); Growth at 900°C. Growth rate 1.5nm/min. Film thickness = 150 nm

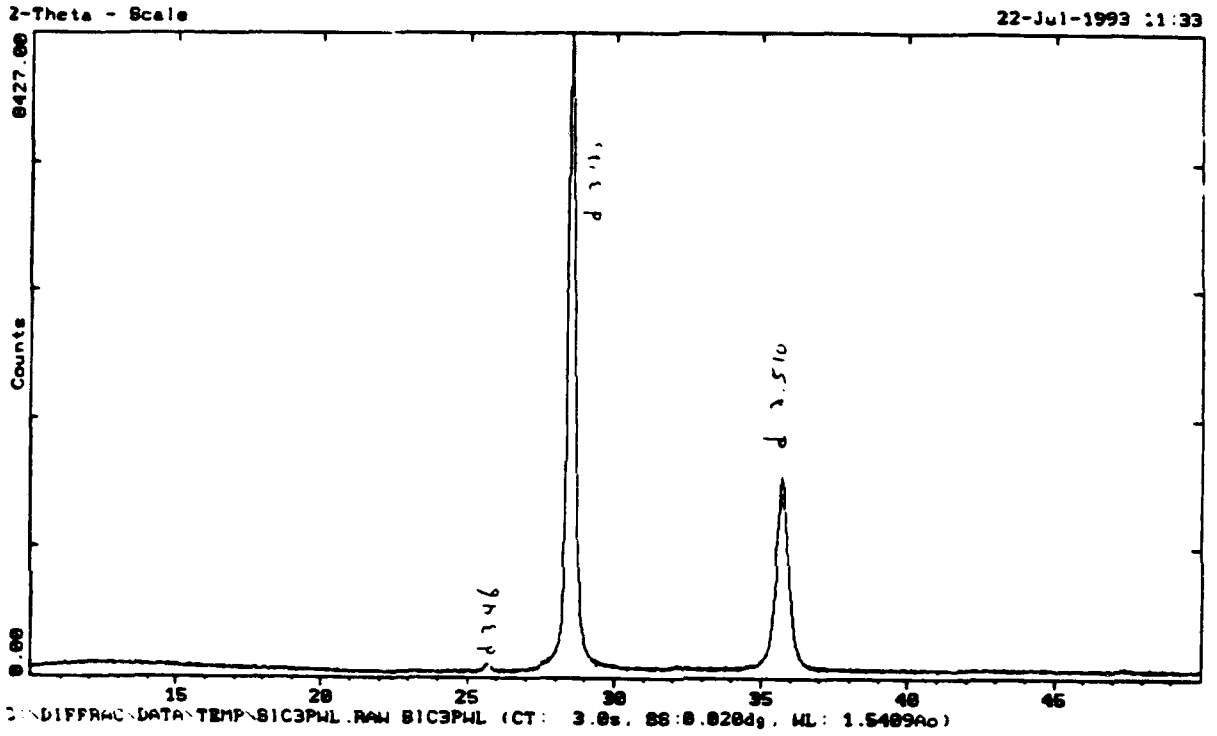

Appendix A

Appl. Phys. Lett.
Submitted 8/93

ATOMIC LAYER EPITAXY OF Si ON Ge(100) USING Si_2Cl_6 AND ATOMIC HYDROGEN

D. D. Koleske and S. M. Gates
IBM T. J. Watson Research Center, Yorktown Hts., NY 10598

ABSTRACT

The surface composition is measured during atomic layer epitaxy (ALE) growth of Si On Ge(100) using Si_2Cl_6 and atomic hydrogen (H_{at}) at $T_S = 400^oC$. During each Si_2Cl_6 exposure, Si is adsorbed until Cl fully terminates the surface, making the Si deposition step self-limiting. The terminating Cl layer is removed by H_{at} exposure. At 400°C, H_2 rapidly desorbs from Ge(100) and Si/Ge alloy surfaces, regenerating the surface dangling bonds for the next Si_2Cl_6 adsorption cycle. A thin alloy is grown epitaxially on the Ge(100) substrate, which displays a linear increase in Si content and a linear decrease in Ge content, measured over 1-20 Si ALE cycles

PACS numbers : 68.55.Ln , 68.35.Dv , 81.15.Gh , 82.65.Yh

Growth of compound semiconductors and insulators in a self-limiting layer-by-layer fashion is known as Atomic Layer Epitaxy (ALE) {1,2}. To extend ALE concepts to the growth of elemental semiconductors, especially silicon, reaction thermodynamics {3} and growth of thin Si films {4-15} have been studied. Si ALE methods rely on self-limiting adsorption of a silane or chlorosilane followed by regeneration of the surface dangling bonds using various heating methods {5-9}, or chemically using atomic hydrogen {10-13}. Alternatively, high surface temperature (T_S) and delivery of the precursor in pulses (with the pulse time and pressure adjusted so that $\simeq$ 1 monolayer (ML) of Si is grown per pulse) may be used {14,15}. Objectives include fine control over deposited Si thickness, uniformity over large areas, and conformal trench coverage. Potentially successful Si ALE methods may involve self-limiting adsorption of chlorosilanes followed by removal of the Cl layer with H_{at} or other radicals {3,11- 13}. Formation of a self-terminating Cl layer requires the chlorosilane to have a Cl to H ratio $\geq$ 1 {16}. Here, we demonstrate that Si_2Cl_6 forms a self-terminating Cl layer that can be removed using H_{at} and that a constant amount of Si is deposited during each ALE cycle. A Ge(100) substrate and 400°C are used. On Si(100), desorption rates of H_2, HCl and $SiCl_2$ are slower, and the optimum temperature for this process would be $\simeq$ 525°C.

The elemental composition of the surface is measured in real time using a variant of direct recoil (DR) spectroscopy {17,18}, in which recoiled ions are detected {19,20}. Briefly, a 10 keV Na^+ ion beam is pulsed at 50 kHz at an incident angle (α) of 3-35° to the surface plane. A small fraction of the direct recoil particles are ions, which can be mass analyzed by time of flight (TOF) through a "reflectron" energy/time focusing electrostatic analyzer {19,20}. At the recoil angle, Φ, of 60°, the recoiled ions (RI) have kinetic energies of $\simeq$ 400 eV for H and 2.3-2.5 keV for Si and Cl. As shown in Figure 1, these are focused using different reflectron voltages for detection of low mass (0-4 amu, left side) and high mass (10-80 amu, right side) ions. The RI spectra are significantly better mass resolved than neutral recoil spectra. However, unlike recoiled neu-

trals which are proportional to surface coverage, the ion fraction generated depends on the chemical state of the surface {17}. The RI peaks in Figure 1 are asymmetric. The low TOF edge is sharper than the high TOF edge, and this reflects the shape of the primary Na^+ pulse.

The Ge(100) sample preparation (previously described {21}) consists of sputtering at 100°C and annealing at $T_S = 600°C$ until no carbon or oxygen contamination is detected, and sharp streaks and a (2X1) reconstruction is observed by reflection high energy diffraction (RHEED) {22}. A clean Ge(100) RI spectra is shown in Fig. 1(a), where TOF has been transformed to mass and RI intensity is plotted on a Log scale. In Fig. 1(a) all 5 Ge isotopes are resolved, and Ge^{2+} ions are observed at 35-40 amu {23}.

Fig. 1(b) shows the clean surface after dosing with $1x10^{-5}$ torr pressure (P) of Si_2Cl_6 for 3 min. at $T_S = 400°C$. Increases are observed in the Si^+, Cl^+, Cl^{2+} and Na^{2+} ion signals. At $T_S = 400°C$, the surface becomes terminated with 1 monolayer (ML) of Cl. We assume that $\simeq$ 1/3 ML of Si is deposited with each saturation, due to the 1/3 ratio of Si/Cl in the precursor. The adsorbed Cl layer was removed with H_{at}, using $5x10^{-6}$ torr H_2 P and resistively heating a W filament. Fig. 1(c) was measured at $T_S = 200°C$ after dosing with H_{at} for 5 min. at $T_S = 400°C$. In this spectrum the Si^+ and Cl^{2+} signals are 0.25 and 0.08 times their original intensities. The Cl^{2+} signal is used to monitor Cl coverage because the Cl^+ (mass 35) signal is obscured by the Ge^{2+} signal. On Ge(100) at $T_S = 400°C$, HCl desorption is rapid {24}, so Cl removal is primarily via thermal HCl desorption. As the Cl termination is removed, deposited Si and the Ge substrate mix to form an alloy (see below).

The surface coverages of Si, H, and Cl were followed in real time *during the Si_2Cl_6 and H_{at} Si ALE growth sequence.* These measurements are summarized in Fig. 2. The

growth sequence was 3 min. of Si_2Cl_6 exposure ($1x10^{-5}$ torr), 2 min. of pumping, 5 min. of H_{at} exposure ($5x10^{-6}$ torr H_2 and hot filament), and 4 min. of pumping. When Si_2Cl_6 is dosed, both the Si^+ and Cl^{2+} signals increase and remain roughly constant. During exposure to H_{at}, Cl is removed from the surface, and the H^+ signal increases gradually. Once the H_{at} is turned off, H_2 desorbs rapidly {24,25}, regenerating the surface dangling bonds for readsorption of Si_2Cl_6. Note that the Si^+ and Cl^{2+} signals decrease concurrently. This effect is primarily caused by mixing of the Si and Ge, forming an alloy layer with Ge surface termination. Surface segregation of Ge (preferred Ge termination of Si_xGe_{1-x} alloys) is a well known effect, and is driven by minimizing the surface free energy {26,27}. The yield of recoiled ions ("ion fraction") decreases with decreasing Cl coverage, and this is a secondary cause for the decreased Si^+ signal.

One requirement for a Si ALE process is self-terminating adsorption of the precursor, making the growth rate per cycle independent of pressure and exposure time. Fig. 3(a) shows the Si^+ signal for two different Si_2Cl_6 pressures, each dosed for 3 min. followed by evacuation. The Si^+ signals are nearly identical for both pressures. The slow decrease in the Si^+ signal while pumping after the Si_2Cl_6 dose is due to the slow desorption of $GeCl_2$ at 400°C {24}. In Fig. 3(b), the Cl terminated surface was dosed with H_{at} ($5x10^{-6}$ torr H_2 + hot filament) for 5 min. (open squares) and 10 min. (closed circles). Once the Cl terminating layer is removed ($\simeq$ 200 s) the Si^+ signal is constant. This verifies that the Cl removal step is self-limiting, and does not measurably etch the deposited Si. Adsorption of H_{at} and subsequent H_2 desorption at 400°C {24,25} do not change the Si surface concentration.

When Si_2Cl_6 and H_{at} doses are repeated at $T_S = 400°C$, Si is incrementally deposited on Ge(100). This is shown in Fig. 4(a) where the Ge^+ (left axis) and Si^+ (right axis) fraction of the total recoil signal is plotted vs. the number of ALE cycles. Both the linear

decrease in the Ge^+ signal and the linear increase in the Si^+ signal are a clear indication that a constant amount of Si is added to the surface during each ALE cycle.

The epitaxial quality of the deposited Si was examined by RHEED after 10 cycles of Si ALE growth, as shown in Fig. 4(b). The RHEED pattern was measured at low T_S along the {010} aximuth using a primary beam energy of 12 keV. Compared to the clean Ge(100) surface {22}, the RHEED pattern has stronger 1st order diffraction streaks and spots. The emergence of spots, which are a projection of the (111) lattice planes, are an indication of 3D roughening {28}, as expected for Si growth on Ge {21,26,27}. The 1/2 order diffraction streaks characteristic of the (2X1) reconstruction {22} become weaker, probably because the Si/Ge interface is not atomically smooth {13,28}. These two trends, namely the increase in intensity of 1st order diffraction features and the decrease in the intensity from 1/2 order diffraction features are evident to a greater extent in the RHEED patterns measured after 15 and 20 Si ALE cycles (data not shown). For Si ALE on a Si(100) surface using Si_2Cl_6 and H_{at}, RHEED patterns at $T_S = 500^oC$ look identical to clean Si(100) {13}, demonstrating that the roughening observed here is due to Si growth on Ge and not from the Si ALE process.

The self-limiting deposition of a constant amount of Si in each ALE cycle has been demonstrated here. At $T_S = 400^oC$, Si_2Cl_6 decomposes to form 1 ML of monochloride Si-Cl and Ge-Cl species. Formation of a Cl terminating layer prevents further adsorption of Si_2Cl_6 limiting the Si growth rate in this study to 1/3 ML of Si per cycle. The amount of Si deposited can be influenced by the choice of silicon precursor molecule. We have compared the degree of self-limiting adsorption behavior of chlorinated Si precursors {16}. For precursors containing H and Cl, T_S must be selected in order to avoid continuous HCl desorption, which can result in sustained Si adsorption. Use of a fully chlorinated precursor (Si_2Cl_6) simplifies this problem.

Removal of Cl from Si using H_{at} is well known {11-13,29}, but H_{at} can chemically "anneal" the surface {30}, as well. In addition to slow removal of Cl, exposure to H_{at} results in efficient abstraction of chemisorbed H by H_{at} {19}, forming dangling bonds (db). Subsequent H_{at} adsorption on these db is exothermic, and the Ge-H or Si-H bond energy must be dissipated by the surface lattice. Enhanced rates of ordering and mixing of the Si/Ge alloy then result from exposure to H_{at}.

We have shown how the elemental surface coverages change during a Si ALE process consisting of alternating exposures of Si_2Cl_6 and H_{at} at 400°C. To verify the deposition of Si, a Ge(100) surface was used. The deposited Si signal is independant of Si_2Cl_6 pressure (Fig. 3) and the Si^+ signal increases linearly as a function of ALE cycles (Fig. 4), indicating that Si is grown on the Ge(100) surface in a truly self-limiting growth process.

Acknowledgements

We thank J.A. Schultz for experimental assistance and helpful discussions. This work is supported by the Office of Naval Research under contract # N00014-91-C-0080.

REFERENCES

1. T. Suntola and M. Simpson, (Eds.); "Atomic Layer Epitaxy", Chapman and Hall, New York, 1990; copyright 1990 by Blackie and Son, Ltd., London.
2. C.H.L. Goodman and M.V. Pessa; J. Appl. Phys. **60** R65 (1986).
3. S.M. Gates; J. Phys. Chem. **96**, 10439 (1992).
4. see Proceedings from the 2nd International Atomic Layer Epitaxy Symposium, Rayleigh, NC, USA, June 2-5, 1992; in Thin Solid Films **225**, 1 (1993).
5. D. Lubben, R. Tsu, T.R. Bramblett and J.E. Greene, J. Vac. Sci. Tech. A **9**, 3003 (1991).
6. Y. Takahashi and T. Urisu; Jpn. J. Appl. Phys. **30**, L209 (1991).
7. S. Imai, S. Takagi, S. Sugiura, M. Matsumura; Jpn. J. Appl. Phys. 1 **30**, 3646 (1991).
8. J. Murota, M. Sakuraba, S. Ono; Appl. Phys. Lett. **62**, 2353 (1993).
9. A. Mahajan, J. Irby, D. Kinosky, R. Wian, S. Thomas, S. Banerjee, A. Tasch, and T. Picraux; Thin Solid Films **225**, 177 (1993).
10. J.A. Yarmoff, D.K. Shuh, T.D. Durbin, C.W. Lo, D.A. Lapiano-Smith, F.R. McFeely, and F.J. Himpsel; J. Vac. Sci. Technol. A **10**, 2303 (1992).
11. J.T. Yates, Jr., C.C. Cheng, Q. Gao, M.L. Colainni, W.J. Choyke; Thin Solid Films **225**, 150 (1993).
12. S. Imai, T. Iizuka, O. Sugiura and M. Matsumura; Thin Solid Films **225**, 168 (1993).
13. D.D. Koleske and S.M. Gates; J. Appl. Phys., in press for 9/93.
14. J. Nishizawa, K. Aoki, S. Suzuki, and K. Kikuchi; J. Electrochem. Soc. **137**, 1898 (1990).
15. F.G. McIntosh, P.C. Colter, and S.M. Bedair; Thin Solid Films **225**, 183 (1993).
16. D.D. Koleske, S.M. Gates and D.B. Beach; Appl. Phys. Lett. 61, 1802 (1992).
17. W. Eckstein; Nuclear Instr. Meth. **B27**, 78 (1987).
18. J.W. Rabalais; Science **250**, 522 (1990), and J.W. Rabalais, CRC Crit. Rev. Solid State Mater. Sci. **14**, 319 (1988).
19. D.D. Koleske, S.M. Gates and J.A. Schultz; J. Chem. Phys., in press.
20. K. Eipers Smith, K. Waters, J.A. Schultz; J. Amer. Ceram. Soc. **76**, 284 (1993).
    J.A. Schultz and H.K. Schmidt; U.S. Patent 5,087,815 (1992).
21. S.M. Gates, D.D. Koleske, J.R. Heath, and M. Copel; Appl. Phys. Lett. **62**, 510 (1993).
22. L.Y.L. Shen; Surf. Sci. **47**, 685 (1975).
23. The increase in multiply charged ions as a function of incident beam energy is discussed in Ref. 17.

24. The TPD peak temperatures for HCl and $GeCl_2$ desorption from Ge(100) are 300°C and 400°C, respectively, see S.M. Cohen, T.I. Hukka, Y.L. Yang and M.P. D'Evelyn; Thin Solid Films **225**, 155 (1993). Slightly higher TPD peak temperatures are observed for mixed Si_xGe_{1-x} alloy surfaces. See (25).

25. B.M.H. Ning and J.E. Crowell; Appl. Phys. Lett. **60**, 2914 (1992).

26. P.M.J. Maree, K. Nakagawa, F.M. Mulders, and J.F. van der Veen; Surf. Sci. **191**, 305 (1987).

27. D.S. Lin, T. Miller, T.C. Chiang; Phys. Rev. B **47**, 6543 (1993).

28. W.K. Liu, S.M. Mokler, N. Ohtani, C. Roberts, B.A. Joyce; Surf. Sci. **264**, 301 (1992).

29. C.C. Cheng, S.R. Lucas, H. Gutleben, W.J. Choyke, and J.T. Yates, J. Am. Chem. Soc. **114**, 1249 (1992).

30. H. Shirai, D. Das, J.-I Hanna, and I. Shimuzu; Appl. Phys. Lett. **59**, 1096 (1991); G. Parsons, J.J. Boland, and J.C. Tsang; Jpn. J. Appl. Phys. **31**, 1943 (1992).

FIGURE CAPTIONS

FIGURE 1. Recoil ion spectra measured from Ge(100) surface using a 10-keV Na^+ beam, with incident angle, α, of 3° with respect to the surface plane and a recoil angle, Φ, of 60°. Low mass spectra (1-4 amu, left side of figure) were obtained using lower reflection grid voltages (see {19}) than for the high mass spectra (5-80 amu). This figure shows the changes in the elemental surface conposition after dosing (a) clean Ge(100) with (b) a saturation dose of Si_2Cl_6, followed by (c) a dosing with H_{at}. Note that the intensity is plotted on a LOG scale.

FIGURE 2. Normalized recoil ion signal for (a) Si^+, (b) H^+, and (c) Cl^{2+} measured during the Si ALE growth cycle. The gas exposures and pump times are; Si_2Cl_6 at $1x10^{-5}$ torr for 3 min., 2 min. pump cycle, H_{at} at $5x10^{-6}$ torr for 5 min., and 4 min. pump cycle. The maximum hydrogen coverage in (b) is $\simeq 0.2$.

FIGURE 3. Plot of the normalized Si^+ ion signal as a function of time for (a) two different Si_2Cl_6 pressures, and (b) two different H_{at} exposures. In (a) the time between the dashed lines indicates the 3 min. Si_2Cl_6 dosing time, after which the Si_2Cl_6 is pumped away. In (b) the Cl terminated surface is exposed to a 5 min. (open squares) and 10 min. (closed circles) H_{at} ($5x10^{-6}$ torr). Note that in both (a) and (b) the final Si^+ signal for each set of conditions is approximately the same.

FIGURE 4. Determination the chemical (a) and structural (b) composition of the deposited Si on Ge(100). (a) plot of the Ge^+ (closed circles) and Si^+ (open squares) fraction of the total recoil ion signal as a function of ALE cycles number. Both signals follow linear dependences on ALE cycle number. (b) RHEED pattern after 10 ALE cycles, measured along the {010} direction using a 12 keV beam energy.

Figure 1

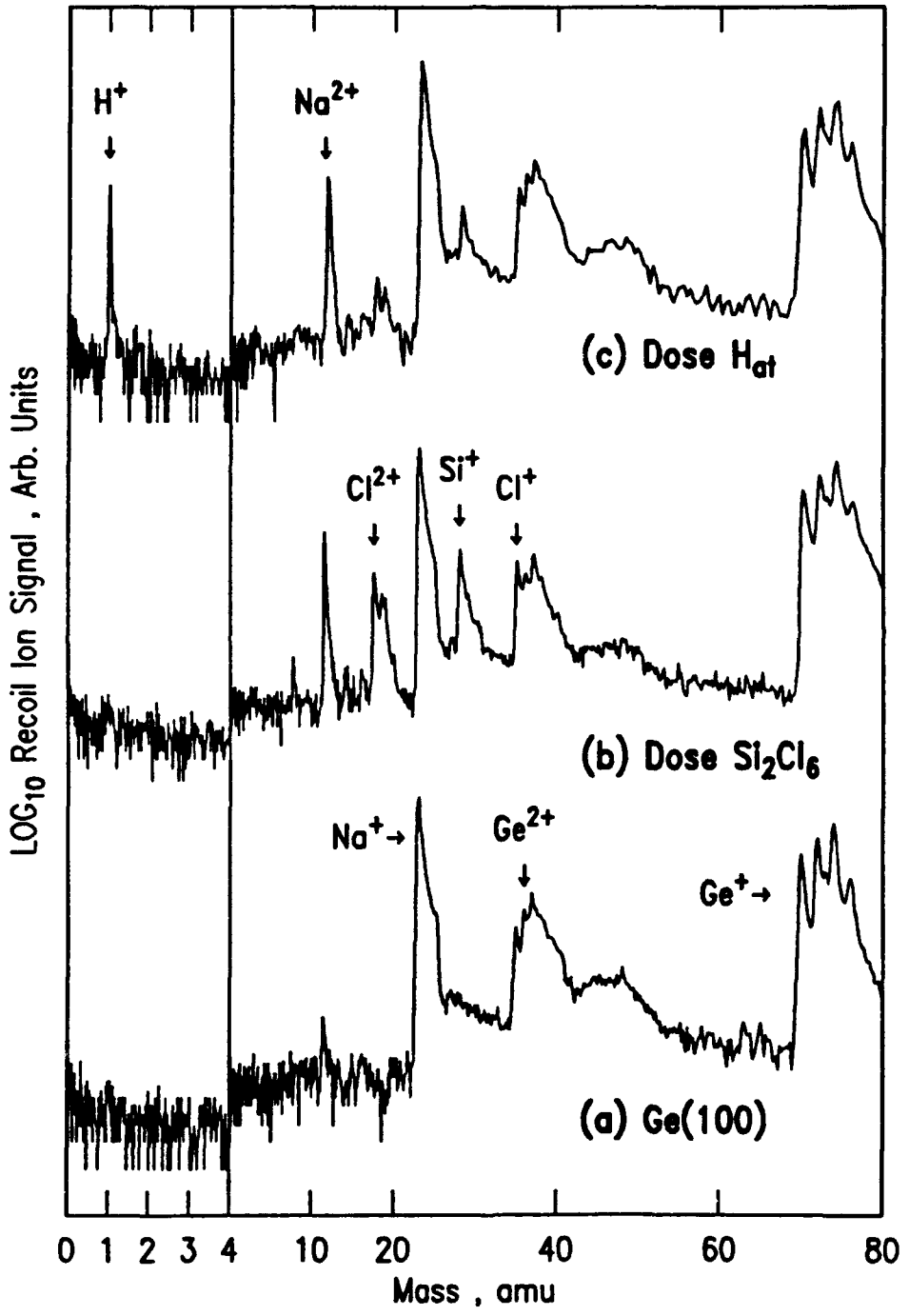
H+
Na2+
(c) Dose Hat
Cl2+
Si+
Cl+
(b) Dose Si2Cl6
Na+→
Ge2+
Ge+→
(a) Ge(100)
LOG10 Recoil Ion Signal , Arb. Units
0 1 2 3 4 10 20 40 60 80
Mass , amu

Figure 2

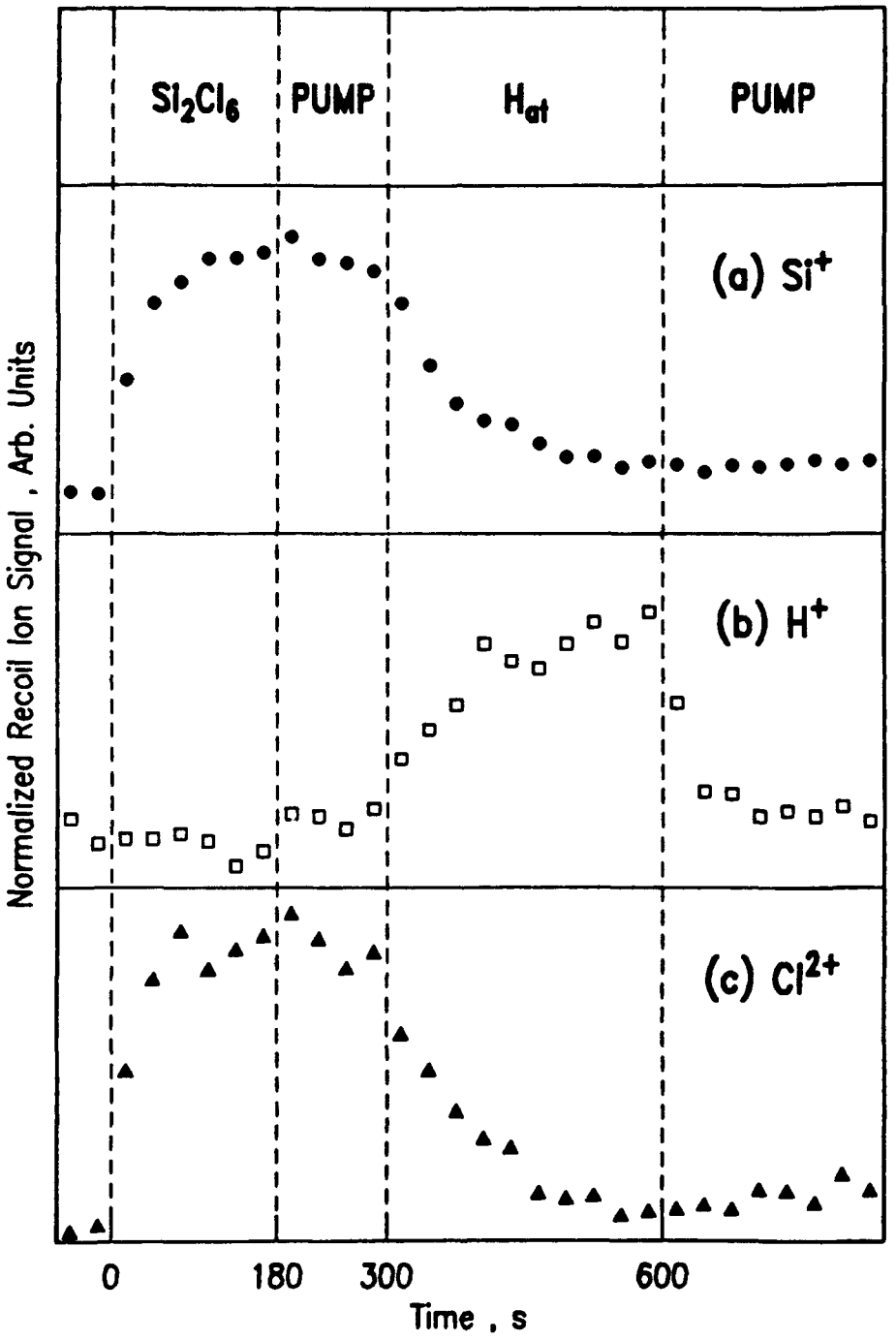
Si_2Cl_6
PUMP
H_{at}
PUMP
(a) Si^+
(b) H^+
(c) Cl^{2+}
Normalized Recoil Ion Signal , Arb. Units
0
180
300
600
Time , s

Figure 3

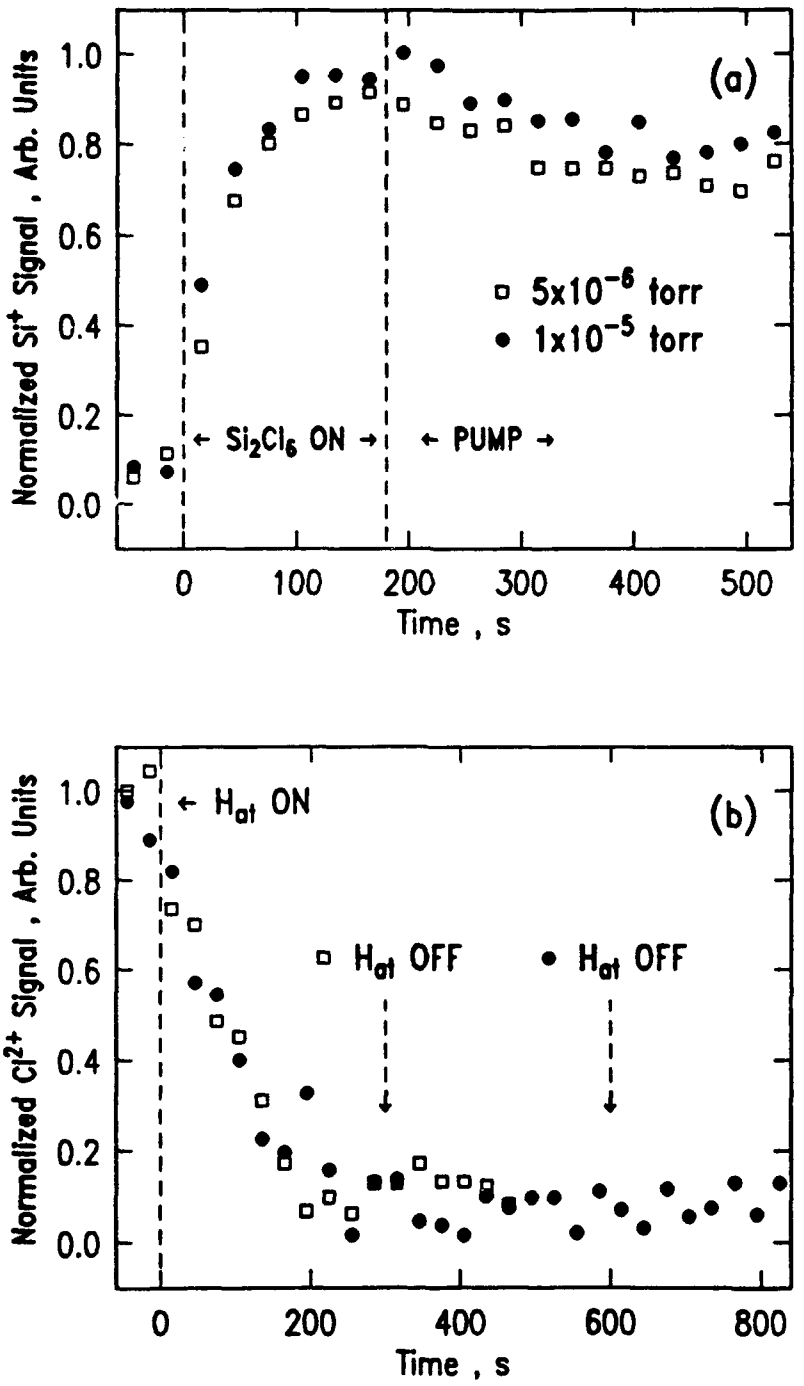
Normalized Si+ Signal , Arb. Units
1.0
0.8
0.6
0.4
0.2
0.0
(a)
5x10−6 torr
1x10−5 torr
← Si2Cl6 ON →
← PUMP →
0
100
200
300
400
500
Time , s
Normalized Cl2+ Signal , Arb. Units
1.0
0.8
0.6
0.4
0.2
0.0
← Hat ON
(b)
Hat OFF
Hat OFF
0
200
400
600
800
Time , s

Figure 4A

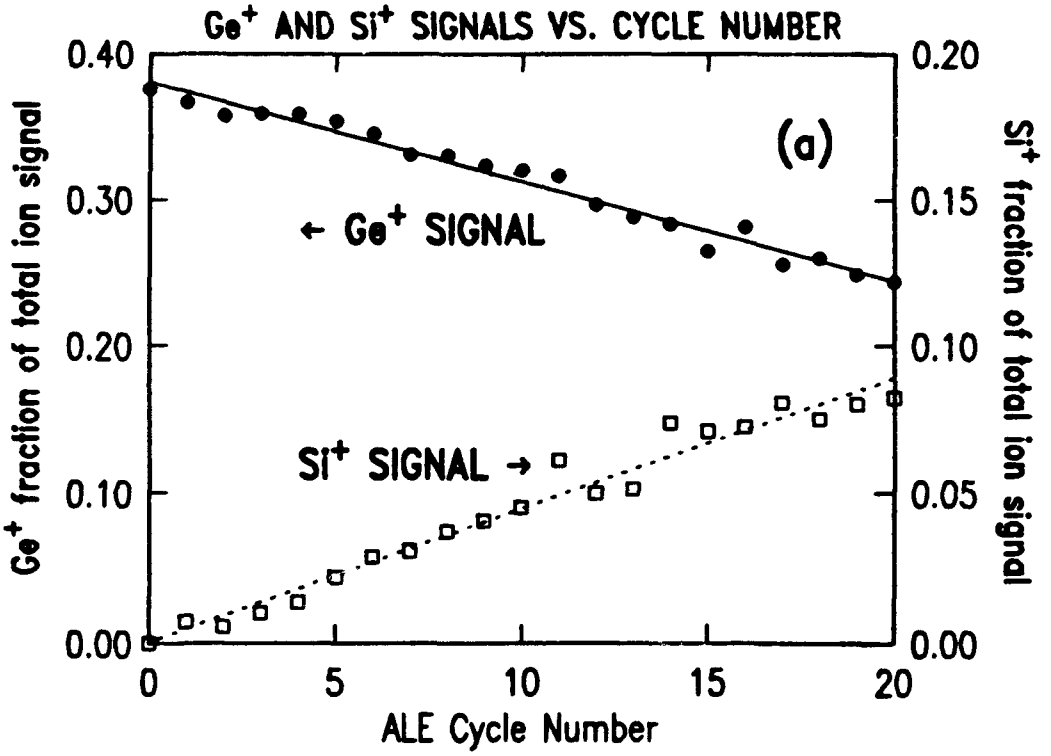
Ge+ AND Si+ SIGNALS VS. CYCLE NUMBER
(a)
← Ge+ SIGNAL
Si+ SIGNAL →
Ge+ fraction of total ion signal
Si+ fraction of total ion signal
0.40
0.30
0.20
0.10
0.00
0.20
0.15
0.10
0.05
0.00
0
5
10
15
20
ALE Cycle Number

Figure 4B

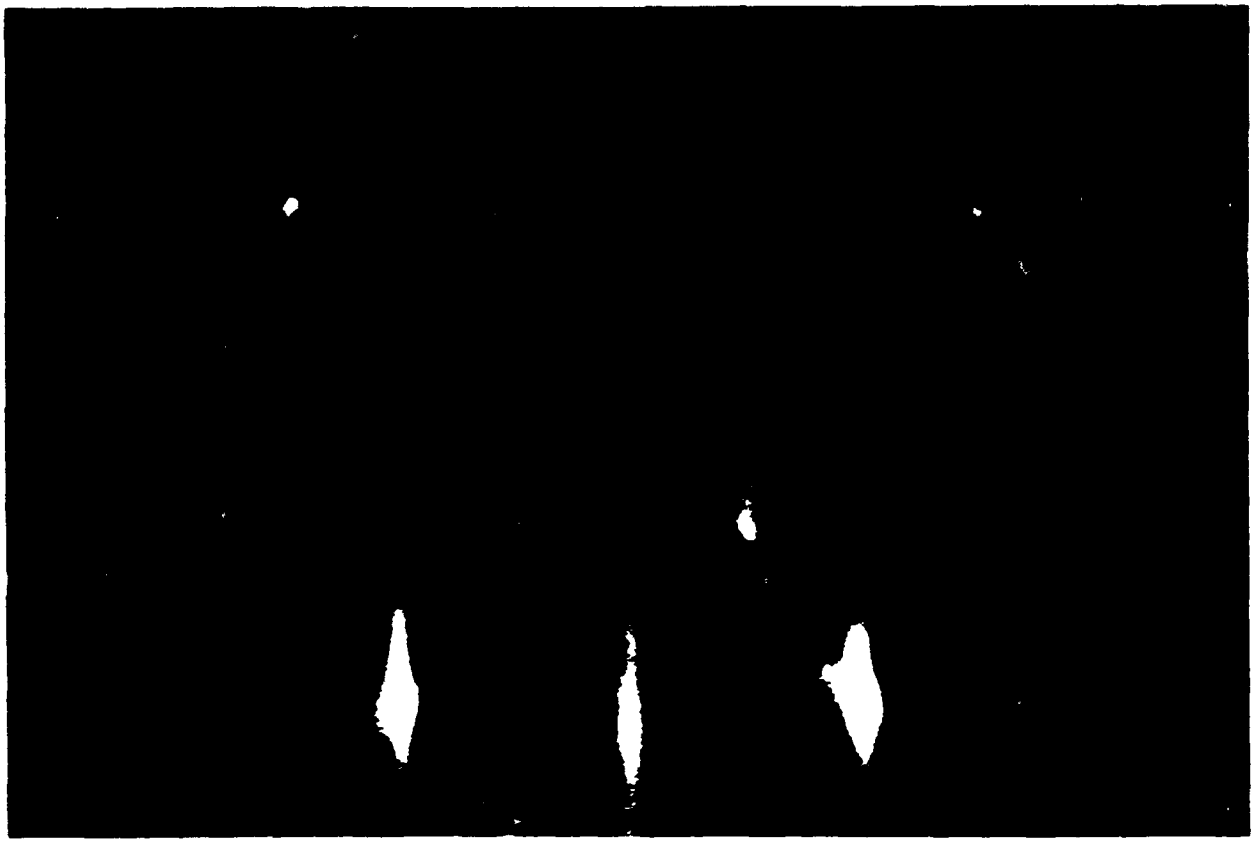

Facile abstraction of chemisorbed D on Si(100) by atomic H

D. D. Koleske and S. M. Gates
IBM, Thomas J. Watson Research Center, Yorktown Heights, New York 10598

J. A. Schultz
Ionwerks, Suite 255, 2472 Bolsover, Houston, Texas 77005

(Received 7 June 1993; accepted 28 July 1993)

The abstraction of chemisorbed deuterium (D) on Si(100) by atomic hydrogen (H_{at}) is studied in real time. The surface H and D coverages are measured by mass analyzing the recoiled H^+ and D^+ ion signals during the abstraction reaction. We find that H_{at} efficiently removes adsorbed D on Si(100) with a low activation energy of 0.8 ± 0.6 kcal/mol and a reaction probability that is 0.36 times the H_{at} adsorption rate on clean Si(100).

Reaction (1) is generally presumed to accurately describe the adsorption of atomic hydrogen (H_{at}) on Si surface dangling bonds (denoted by _–Si).

$$H_{at} + \_\text{–Si} \rightarrow \text{H–Si}. \quad (1)$$

The literature on H_{at} + Si typically ignores the abstraction of chemisorbed H by H_{at} incident from the gas phase, reaction (2):

$$H_{at} + \text{H–Si} \rightarrow H_2(g) + \_\text{–Si}. \quad (2)$$

Reaction (2) has been inferred to occur on H/Si(100)[1] and has been observed by mass spectrometry using amorphous hydrogenated Si.[2] Reaction (2) is roughly 1 eV exothermic (see below), and may occur either via an Eley–Rideal or a "hot precursor"[3] mechanism. Reactions (1) and (2) have practical consequences in the growth of amorphous hydrogenated Si[4] and fine grain polycrystalline Si[5] using SiH_4 or H_2 plasmas. We demonstrate here that abstraction [reaction (2)] occurs with a probability of about 0.36 times that of reaction (1), and reaction (2) always accompanies reaction (1) when Si surfaces are exposed to H_{at}.

The abstraction rate of chemisorbed D by H_{at} on Si(100) is measured using a variant of direct recoil (DR) spectroscopy in which recoiled ions are mass analyzed by time of flight (TOF) through a "reflectron" energy/time focusing electrostatic analyzer.[6,7] Briefly, a 10 keV Na^+ ion beam is pulsed at 50 kHz and impinged at an incident angle (α) of 15° on the Si(100) surface. The reflectron TOF analyzer is located at a recoil angle, Φ, of 60°. Using this detection scheme, the H^+ and D^+ recoil ion signals can be clearly resolved as shown in Fig. 1. DR spectroscopy has been reviewed[8,9] and it is well known that the recoiled ion fractions can depend on the chemical state of the surface. Here, we are exchanging H for D so that the chemical composition of the surface is not changing, and we make the assumption that the recoiled ion signals are proportional to surface coverage. Neutral DR signals are known to obey this proportional relationship.[10,11]

The Si surfaces are prepared and cleaned as previously described.[11] H_{at} and D_{at} are generated by dissociating H_2 or D_2 on a hot filament ($T \approx 2000$ K).[12] The initial surface containing 1 monolayer (ML) of D is prepared by dosing clean Si(100) with 5×10^{-7} Torr of D_2 under a hot filament at a surface temperature (T_S) of 425 °C for 5 minutes (see Fig. 1).[13–15] The surface containing 1 ML of D is exposed to H_{at} and simultaneously a series of TOF spectra are collected. The coverages of H (θ_H) and D (θ_D) are determined by integrating the H^+ and D^+ ion signals and dividing by the integrated signal from surfaces containing 1 ML of H or D. The Na^+ beam current measured at the crystal is 0.1 nA, which in 1000 s corresponds to a Na^+ dose of ≈ 0.01 ML.

A series of TOF spectra is shown in Fig. 1 (each signal averaged for 30 s) for the removal of chemisorbed D on Si(100) by H_{at}. Initially, the surface is D covered [Fig. 1(A)], and example spectra are shown after dosing with

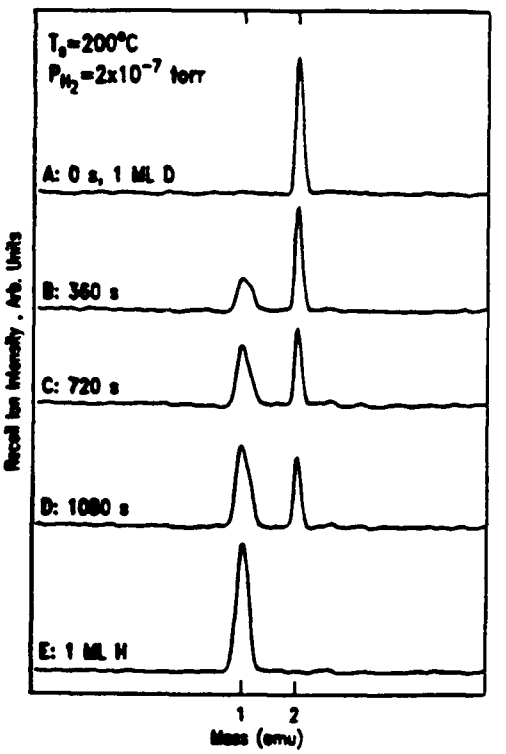

FIG. 1. A series of time-of-flight recoiled ion spectra showing H_{at} removal of D on Si(100). (A) 1 monolayer (ML) of D on Si(100). (B)–(D): this surface after 360, 720, and 1080 s of H_{at} exposure. (E): 1 ML of H on Si (100). Details are given in the text.

 0021-9606/93/99(7)/5619/4/$6.00

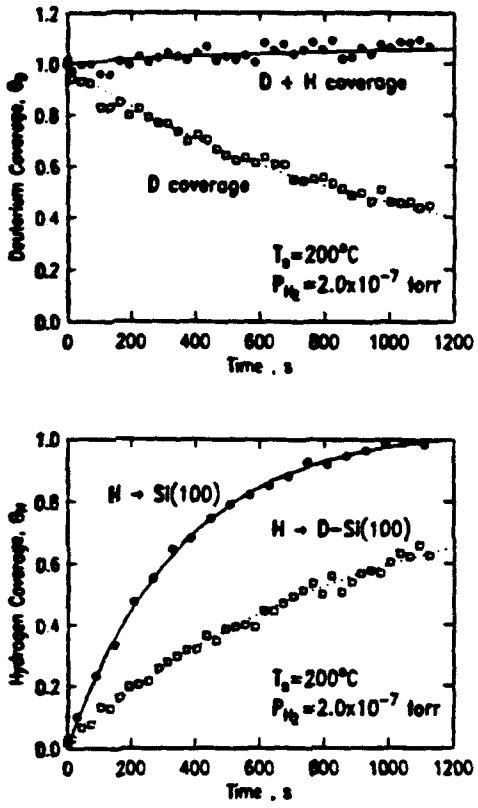

FIG. 2. Top panel: Deuterium coverage during dosing with H_{at} with a H_2 pressure of 2.0×10^{-7} Torr at T_S=200 °C (open squares, dashed line). The initial deuterium coverage is 1. The total deuterium and hydrogen coverage under these conditions is also plotted (filled circles, solid line). Bottom panel: Hydrogen coverage during dosing with H_{at} on clean Si(100) (filled circles, solid line) and on D covered Si(100) (open squares, dashed line) as a function of time. The solid and dashed lines are fits to Eq. (3) as described in the text.

2.0×10^{-7} Torr of H_2 and a hot filament for various times [see Figs. 1(B), 1(C), and 1(D)] at T_S=200 °C. For comparison a 1 ML H terminated Si(100) surface is shown in Fig. 1(E). The relative shape of the H and D DR ion peaks is due solely to the reflectron focusing voltages, which were chosen to *maximize both H^+ and D^+ ion signals*.

Figure 2 is derived from Fig. 1 and illustrates the surface H and D coverage vs time. The θ_H and θ_D values shown in Fig. 2 are the average of four independent measurements under identical conditions. The top panel shows both the decrease in θ_D vs time, and the total H and D coverage during the experiment. The latter increases to 1.06 ML after 1200 s of H_{at} exposure. In the bottom panel of Fig. 2, θ_H is plotted vs time during the removal of D from the surface (open squares). Adsorption of H on clean Si(100) (closed dots) is shown in the bottom panel measured using identical conditions. Concerning reaction of H_{at} with the clean surface, Eqs. (1) and (2) give the complete mechanism. The solid line is a fit to the clean surface data with the time dependence of θ_H given by Eq. (3). Here, t is time, θ_S is the coverage of sites for H, $a=(\theta_S k_1)/(k_1+k_2)$ and $b=F_H(k_1+k_2)$. The values a=1.036 and $b=2.82\times10^{-3}$ s^{-1} yield the solid line:

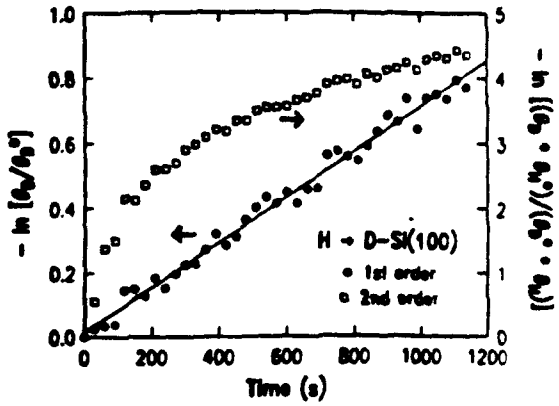

FIG. 3. Order plots for H_{at} removal of D on Si(100), with a pseudo-first-order, $-\ln(\theta_D/\theta_D^0)$, rate law plotted using solid dots (left ordinant) and a pseudo second order, $-\ln(\theta_H^0\theta_{D'}/\theta_H^0\theta_{D'})$, rate law plotted using open squares (right ordinant). The solid line is a fit to the 1st order rate law (solid dots).

$$\theta_H = a^*(1-\exp(bt)). \tag{3}$$

At very short times, reaction (2) is neglected and the initial slope is the rate of reaction (1).

Reaction of H_{at} with the D terminated surface is described by Eqs. (1), (2), and (4):

$$H_{at} + \text{D-Si} \rightarrow \text{HD}(g) + \_\text{-Si}. \tag{4}$$

The open squares in Fig. 2 can be fit with a solution resembling Eq. (3), but containing a sum of 2 exponential terms as will be reported elsewhere.[16] At very short times, reaction (2) can be neglected and the H_{at}+D terminated Si case is described by equations (1) and (4). The *initial slopes* of the dots and squares ($t<100$ s) compare the rate of H_{at} adsorption on the two surfaces. Adsorption of H_{at} on the D covered surface is 0.36 times the rate for H_{at} adsorption on the clean surface. This is close to the estimated value of Sinniah and co-workers of 0.4.[1] At longer times as θ_H increases, reaction (2) occurs simultaneously with reaction (4).

We have analyzed the D removal kinetics shown in Fig. 2 using two different rate laws as shown in Fig. 3. For pseudo-first-order removal of D, a plot of the quantity $-\ln(\theta_D/\theta_{D'})$ vs time should be linear, while for a pseudo-second order removal of D, a plot of the quantity $-\ln(\theta_D\theta_{H'}/\theta_H\theta_{D'})$ vs time should be linear.[17] The superscript zero denotes the initial (time zero) coverage, which for $\theta_{D'}=1$ and for $\theta_{H'}=0.018$ determined from Fig. 2. These two plots are shown in Fig. 3 for a pseudo-first (solid dots) and pseudo-second (open squares) order rate laws. The first-order rate law fits the data well, and the slope of the solid line is the pseudo-first-order rate constant, k_{p1}. A pseudo-first-order rate law was determined by Sinniah and co-workers for H_{at} abstraction of D on Si(100).[1]

The quantity $\ln(k_{p1})$ is plotted in Fig. 4 as a function of $1/T_S$, using a constant H_{at} flux (3.0×10^{-7} Torr of H_2). From this Arrhenius plot we measure an activation energy, E_A, of 0.6±0.2 kcal/mole. This E_A is similar to the 0.7

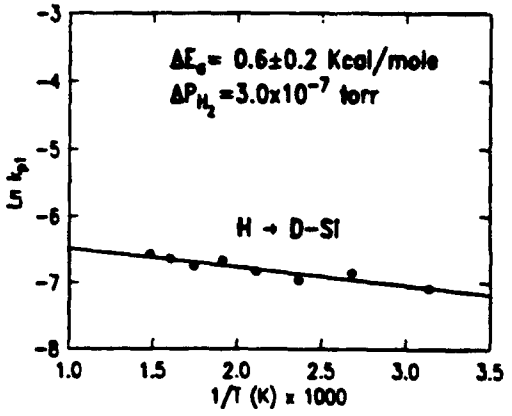

FIG. 4. An Arrhenius plot of the D removal rate, ln (k_{d1}) vs $1/T_S$, measured using 3.0×10^{-7} Torr H_2. An activation energy of 0.6 ± 0.2 kcal/mole is measured for D removal on Si(100) using H_{at}.

±0.6 kcal/mole measured by us[11] and 1.6 kcal/mole measured by Cheng *et al.*[18] for Br removal on Si(100) using H_{at} for T_S below 400 °C. This low E_A indicates adsorbed D is removed from the surface via an activationless mechanism. This seems reasonable considering the exothermicity of reactions (1) and (2). The surface monohydride Si–H bond energy is $\simeq$81 kcal/mole[19] and the H–H bond energy is 104 kcal/mole.[20] Using these bond energies to estimate the enthalpy change (ΔH), reaction (1) has a ΔH of $\simeq-81$ kcal, and reaction (2) has a ΔH of $\simeq-23$ kcal/mole. The total ΔH for (1) followed by (2) is rigorously -104 kcal/mole, because the sum of reactions (1) and (2) is $2\ H_{at}\rightarrow H_2$, and the Si surface is simply a catalyst for H recombination.

We have studied reflection high energy electron diffraction (RHEED) patterns of the D-terminated surface [Fig. 1(A)], and of this surface after H_{at} exposure. No change in the pattern is observed for the total accumulated H_{at} exposures used here. As reported elsewhere, roughening of the surface is detected for H_{at} exposures that are 60 times higher than the exposures used in Figs. 1–3.[21]

We have shown that H_{at} efficiently removes adsorbed D on Si(100), however the mechanism for D removal is not clear. Four observations are pertinent to the mechanism. First, no change in the first order rate law is observed over the course of the experiment in Fig. 3. This indicates there is no substantial change in the reaction mechanism *or the rate* as the total H_{at} exposure increases. Second, the efficiency of D removal is high. On the D-saturated surface, H adsorbs with 0.36 times the rate of adsorption on the clean surface. The latter can be estimated to occur with a sticking probability in the range 0.2 to 1.[22] Thus the absolute probability of D removal is in the range 0.06–0.36. Third, the near zero activation energy indicates removal by an activationless mechanism. Fourth, no evidence of surface roughening is seen by RHEED for H_{at} exposures that remove 0.6 ML of adsorbed D.

Removal of D by formation of silicon hydride etch products ($SiDH_x$, $x=2$ or 3) is a possible mechanism. Etching of the Si surface occurs through the sequential insertion of H_{at} into Si–Si surface bonds.[23] and for each insertion $\Delta H\simeq-30$ to 35 kcal/mole.[11] This mechanism is not activated, but requires exposures of H_{at} that are higher than those used here. The accumulated H_{at} exposure at the end of a D removal experiment (Figs. 1–3) corresponds to the minimum exposure needed to detect etching.[23] No etch products are detected for lower H_{at} exposures.[23] Also, the rate of D removal by etching should depend on the total H surface coverage. This rate should change during the course of our experiments if etching is involved, yet no change in the rate is observed. At the end of our experiments, the total surface coverage ($\theta_H+\theta_D$) has increased by 0.06 of the initial $\theta_D=1.0$ ML (see Fig. 2, top panel). The coverage of surface dihydride species is estimated to linearly increase from 0 to 0.06 ML during the experiment. Trihydride species are less stable than dihydride, and trihydrides are the probable etching precursor.[23,24] With less than 0.06 of the surface being dihydrides, the trihydride coverage should be $\simeq$0.01 ML, or less, too small a coverage to account for a 60% decrease in θ_D occurring with an absolute probability on the order of 0.06–0.3. Recently, Dobbs and Doren have used the reaction of H_{at} with Si_2H_6 in a theoretical study to compare the activation barriers for H_{at} to abstract H and to remove SiH_3 (forming SiH_4).[24] This work compares the reactivities of Si–H and Si–Si bonds towards H_{at}, and views Si_2H_6 as a model system for the surface reaction. Abstraction was found to have the lower barrier.[24] If etching contributes to the D removal seen in Figs. 1–3, we think it is a very minor component.

We believe the removal of adsorbed D using H_{at} probably occurs via a generalized Eley–Rideal (ER) abstraction,[3] where gas phase or partially accommodated H_{at} collides with adsorbed D to form HD. Accommodation of H_{at} into a loosely bound mobile precursor state ("hot" precursor) could occur via elastic scattering or phonon creation. As discussed by Kasemo and Harris, such a mechanism could follow either first or second order kinetics depending on the extent of H_{at} accommodation and other factors.[3] In a "hot" precursor state, H_{at} is not fully accommodated to T_S so that translationally and internally excited reaction products could be generated.[3] For abstraction of D by H_{at} on Cu(100), Rettner has measured product HD translational energies that are $\simeq$40% of the H–D bond energy.[25] Quantum mechanical studies by Jackson and Persson (J&P) suggest that H_{at} removal of adsorbed H and D on Cu produces vibrationally excited H_2 or HD with population of $v=4$ to $v=6$.[26] These authors find isotope effects due to the mass difference between H and D.[26] Compared to the H_{at} removal of D we report here, D_{at} removal of adsorbed H on Si(100) is more efficient,[19] as predicted by the J&P model.[26]

In summary, we have measured kinetics for H_{at} abstraction of chemisorbed D, forming HD, on Si(100) for the first time. We find that D removal is pseudo-first order, with a measured activation energy of 0.6 ± 0.2 kcal/mole. By comparing the initial slopes (near zero time) for H adsorption on clean Si(100) and D covered Si(100), we measure a reaction probability for $H_{at}+D\text{–}Si(100)-HD+\_-Si(100)$ [reaction (2)] that is 0.36 times that of

H_{ad}^{+} $-Si(100) \rightarrow H-Si(100)$ [reaction (1)]. Our results demonstrate that H_{ad} removal of adsorbed D is ≈ 6 times more efficient than Br removal on Si. Future studies will focus on the isotope effects on the abstraction rate.[16]

This work is supported by the Office of Naval Research under Contract No. N00014-91-C-0080.

[1] K. Sinniah, M. G. Sherman, L. B. Lewis, W. H. Weinberg, J. T. Yates, Jr., and K. C. Janda, J. Chem. Phys. 92, 5700 (1990).
[2] J. R. Abelson, J. R. Doyle, L. Mandrell, A. M. Myers, and N. Maley, J. Vac. Sci. Technol. A 8, 1364 (1990).
[3] J. Harris and B. Kasemo, Surf. Sci. 105, L281 (1981).
[4] H. Shirai, D. Das, J.-I. Hanna, and I. Shimizu, Appl. Phys. Lett. 59, 1096 (1991).
[5] S. Veprek, Pure Appl. Chem. 54, 1197 (1982).
[6] J. A. Schultz and H. K. Schmidt, U.S. Patent 5,087,815, 1992.
[7] K. Eipers Smith, K. Waters, and J. A. Schultz, J. Am. Ceram. Soc. 76, 284 (1993).
[8] W. Eckstein, Nucl. Instrum. Methods B 27, 78 (1987).
[9] J. W. Rabalais, Science 280, 522 (1990); J. W. Rabalais, CRC Crit. Rev. Solid State Mater. Sci. 14, 319 (1988).
[10] J. N. Chen, H. Kang, and J. W. Rabalais, J. Am. Chem. Soc. 109, 5020 (1987).
[11] D. D. Koleske and S. M. Gates, J. Chem. Phys. (to be published).
[12] T. Sakurai, M. J. Cardillo, and H. D. Hagstrum, J. Vac. Sci. Technol. 14, 397 (1977).
[13] K. Oura, J. Yamane, K. Umezawa, M. Naitoh, F. Shoji, and T. Hanawa, Phys. Rev. B 41, 1200 (1990).
[14] Y. J. Chabal and K. Raghavachari, Phys. Rev. Lett. 53, 282 (1984).
[15] J. J. Boland, Surf. Sci. 261, 17 (1992).
[16] D. D. Koleske and S. M. Gates (in preparation).
[17] J. I. Steinfeld, J. S. Francisco, and W. L. Hase, *Chemical Kinetics and Dynamics* (Prentice-Hall, Englewood Cliffs, 1989).
[18] C. C. Cheng, S. R. Lucas, H. Gutleben, W. J. Choyke, and J. T. Yates, J. Am. Chem. Soc. 114, 1249 (1992).
[19] M. P. D'Evelyn, Y. L. Yang, and L. F. Sutcu, J. Chem. Phys. 96, 852 (1992); C. J. Wu and E. A. Carter, Chem. Phys. Lett. 185, 172 (1991); P. Nachtigall, K. D. Jordan, and K. C. Janda, J. Chem. Phys. 95, 8652 (1991); Z. Jing, and J. L. Whitten, Phys. Rev. B 46, 9544 (1992).
[20] W. L. Jolly, *Modern Inorganic Chemistry* (McGraw-Hill, New York, 1984).
[21] D. D. Koleske and S. M. Gates, J. Appl. Phys. (in press).
[22] U. Bischler, P. Sandl, E. Bertel, T. Brunner, and W. Brenig, Phys. Rev. Lett. 70, 3603 (1993).
[23] S. M. Gates, R. R. Kunz, and C. M. Greenlief, Surf. Sci. 207, 364 (1989).
[24] K. D. Dobbs and D. J. Doren, J. Am. Chem. Soc. 115, 3731 (1993).
[25] C. T. Rettner, Phys. Rev. Lett. 69, 383 (1992).
[26] B. Jackson and M. Persson, J. Chem. Phys. 96, 2378 (1992).

ppendix C

Atomic Layer Doping for Silicon

D.A. Grützmacher, S.S. Iyer, K. Eberl, A.R. Powell, T.O. Sedgwick and B.A. Ek

IBM T.J. Watson Research Center, Yorktown Heights, NY 10598, USA

Abstract

We report on initial results of the potential of self limiting surface reactions for the doping of Si layers using Molecular Beam Epitaxy (MBE) and Atmospheric Pressure Chemical Vapor Deposition (APCVD). MBE experiments using Sb as an n-type dopant in a self limiting process is obtained at a coverage of half a monolayer. No evidence of a self limiting process has yet been found for the p-type doping using B_2H_6 above 400°C. In the case of MBE growth at temperatures below 400°C the B is only partly activated (10-20%). In APCVD grown samples B surface coverage leads to significant growth inhibition of the subsequent deposition of Si from $SiCl_2H_2$. Finally, preliminary results of atomic layer doping using AsH_3 in APCVD indicate a self limitation of chemisorption of AsH_3 at about 0.1 monolayer at a temperature of 600°C, however subsequent growth of Si leads to a smearing out of the As due to segregation and to the residence time of As in the system.

A) Introduction

Conventional Si-epitaxy employs ion-implantation for the incorporation of dopants. Excellent dosimetry is achieved by monitoring ion currents. However, implant damage removal requires an annealing process that results in diffusion that may not be acceptable or adequate for future generation device technology.

The degree of reproducibility and control obtained by ion implantation might be hard to meet by conventional growth techniques using in-situ doping, since total doses of often less then 0.1 monolayer to be deposited within a few nm and with a reproducibility of a few % are commonly required for modern bipolar technology. Here we explore the possibility of using self-limiting surface reactions (SLSRs) as a method to meter precise dopant doses for both Si epitaxy and as a diffusion source. SLSRs have been proposed for various Atomic Layer Epitaxy schemes /1/. The incorporation of dopants by SLSR processes is attractive, since no self-passivation at exactly one monolayer is mandatory, which is a general problem in Si Atomic Layer Epitaxy (ALE) processes for Si and SiGe /2/. Conceptually an Atomic Layer Doping (ALD) process with self passivation at a fraction of a monolayer would lead to the incorporation of a reproducible dose of dopant onto a surface. Fig.1 shows the ALD process schematically. When combined with epitaxy, the epitaxial growth is arrested and the growth surface is exposed to the doping constituents. After surface saturation is reached, an extraction process may be needed to renew the growth surface. Thereafter epitaxy is resumed. This cycle may be repeated till the required dose is attained. Very often, stearic hindrance will prevent the adsorption of more than a fraction of a monolayer. ALD may be combined with diffusion as well. Such a process may be used to control source-drain diffusion in CMOS technology. In order to prevent desorption of dopants, a capping layer of silicon nitride or Si may be needed.

B) Experimental

The experiments were performed in a solid source MBE system equipped with a B_2H_6 (1% in H_2) gas source and with an APCVD apparatus using $SiCl_2H_2$, B_2H_6 (0.5% in H_2) and AsH_3 (0.2% in He) as reactive gases in a H_2 carrier. In the case of the MBE system the partial pressure of the B_2H_6 is adjusted manually via a leak valve. A remote ion gauge, which is located to avoid B_2H_6 cracking, measures the leak rate. For the ALD experiments B_2H_6 partial pressures of 10^{-4} Pa and 0.13 Pa have been used in the MBE and APCVD, respectively. ALD of As by APCVD was performed using an AsH_3 partial pressure of 0.13 Pa.

The following growth cycles were used to study the capabilities of the 1)MBE and 2)APCVD for ALD processes:

1) After a growth of a Si-buffer layer the surface was exposed to either B_2H_6:H_2 or Sb during a growth interruption. The growth was interupted for 30 min, allowing 10 min of pumping on the system before and after the exposure. The structures were then capped by a 100 nm thick Si layer. The exposure time and the growth temperature were chosen as growth parameters.

2) Fig.2 shows the growth cycle used for the APCVD experiments. After the growth of a Si layer at 650°C the temperature was dropped within 3 min to the "ALD-temperature" (T_{ALD}).At T_{ALD} the surface was exposed to the dopant and after a purge time of 1 min the temperature was raised again to 650°C for the Si deposition. During the growth interruptions the reactor was purged with hydrogen. Experiments at T_{ALD} of 400°C, 500°C and 600°C were performed. This process was cycled a few times varying the exposure time t_p from 1 to 64 s.

C) Results and Discussion

1) Sb doping in Si MBE

Elemental Sb is the preferred dopant for n-type doping in Si MBE due to the low vapor pressure. Metzger /8/ has studied the adsorption kinetics of Sb on Si (100), (111) and (110) in great detail. On Si (100) the pertinent observations are described with help of Fig. 3 adapted from that work. Sb adsorbs in an ordered superstructure on Si (100). As coverage increases to 0.5 monolayer (ML, $1ML = 1.2x10^{15}$ cm^{-2}) the fractional order LEED diffraction spots are gradually extinguished and a 1x1 reconstruction is obtained. Further adsorption of Sb retains this 1x1 reconstruction till several MLs of Sb are adsorbed.

Thermal desorption spectroscopy shows that below 0.5 ML a single desorption peak is observed at about 950°C. However, as the coverage is increased beyond 0.5 ML an additional desorption peak is observed at about 450°C. All Sb in excess of 0.5 ML desorbs at this temperature.

This suggests that a fixed coverage of exactly 0.5 ML may be easily achieved by exposing the Si (100) surface to an Sb flux in excess of 0.5 ML and desorbing the excess at about 500°C for several minutes. Monitoring the surface reconstruction till a 1x1 reconstruction is obtained and then continuing further exposure for a short time will ensure that the coverage of 0.5 ML is reached. We have used this method to suppress long range order in SiGe alloys /9/. Alternatively, exposure may be performed at substrate temperatures in excess of 500°C and the desorption step may be eliminated as coverage will not exceed 0.5 ML.

While we have now a precise doping source, actual epitaxial doping is made complicated by the tendency of Sb to segregate to the growing surface /10/. To obviate this problem, subsequent Si growth at extremely low temperatures (below

400°C) is required. Alternatively, amorphous film deposition, followed by Solid Phase Epitaxy is needed /11/.

2) B_2H_6 doping in Gas Source MBE

Fig. 4 shows a δ doped layer obtained by exposing a clean 2x1 reconstructed surface to the B_2H_6:H_2 mixture for 10 min at 550°C. Growth was then resumed after pumping on the system for 10 min. The full width half maximum (FWHM) is 4 nm and attests to the sharp profiles possible using this technique. However, no self limitation of the B_2H_6 adsorption is identified for these growth conditions. Fig. 5 shows the boron sheet density obtained from Secondary Ion Mass Spectroscopy (SIMS) as function of the B_2H_6 exposure in experiments similar to the one in Fig. 4. At the low coverage of $5x10^{11}$ to $5x10^{12}$ cm^{-2} shown in Fig. 5 the dependence appears to be linear, however, at higher coverages the net incorporated dopant increases sublinearly. This goes along with a reduction of the sticking coefficient as a function of the boron coverage which is shown in Table I. Clearly it decreases with increasing coverage approaching $3x10^{-4}$ in agreement with the data of Yu et al. /12/. The sticking coefficients were calculated by the total amount of B_2H_6 at the end of the exposure time and the total exposure time, these values may be high, since this calculation averages over the time and does not take the higher sticking coefficient at the beginning of the exposure into account, nevertheless the sticking coefficient does not approach zero. These results in this temperature range suggest that no self limiting reaction occurs. Yu et al. suggest a self limiting adsorption at 10^{14} cm^{-2} if the adsorption is done at very low temperatures (below 200°C). At these temperature the exposure required for achieving this coverage is several thousand Langmuirs, which is beyond our current experimental capabilities. However, we did investigate the activation of boron in our experiments as a function of temperature. For boron incorporated at temperatures above 500°C, the activation was within the limits of the meas-

urement nearly 100%. This number dropped abruptly to below 20% for incorporation at 400°C. Further annealing at 650°C for 30 min did not improve this number significantly. Apparently the boron is passivated when incorporated at low temperatures. Hydrogen bound to the boron, which appears to be likely at low temperatures, might be the reason for the deactivation. However, H is expected to be removed from the B during the anneal leading to a higher activation, which was not observed in the experiment. Further investigations appear to be neccessary for complete understanding of this phenomenon.

3) B_2H_6 doping in APCVD

In contrast to the experiments using the MBE, complex gas phase reactions may occur in APCVD, which complicate the interpretation of the data. After the deposition of Si using $SiCl_2H_2$ the surface is predominantly terminated by $SiCl_x$ species, most likely SiCl /2/. B_2H_6 is rather unstable and it decomposes in the gas phase, the species arriving at the surface are likely reactive BH_x components.

Fig. 6 shows the boron sheet density determined by SIMS in dependence on the exposure time for T_{ALD} = 400°C and 600°C. There is no indication of a saturation effect, in fact the sheet density appears to increase super-linearly in the range of exposure times studied to well past monolayer coverage. For t_p = 64 s the amount of boron deposited is equal to 5 ML of Boron. Apparently, the reactive boron species, possibly the radical BH_3, which arrives at the surface continues to deposit after the first ML. At very low temperatures the gas phase reactions creating these reactive species might be suppressed, but it is very possible that the B_2H_6 molecule will not be adsorbed on the SiCl terminated surface under these conditions.

Fig. 7 shows the dependence of the thickness of the Si cap layer on the boron sheet density determined by SIMS. The data reveal a significant growth

inhibition of Si on heavily B-terminated surfaces. This finding suggests that initially the nucleation of Si from $SiCl_2H_2$ on the B terminated surface is hampered. Surprisingly, this inhibition is found even when the SIMS data reveal a B coverage of much less then one monolayer. We think, that indeed after the exposure to B_2H_6 for a few seconds, the amount of boron on the surface is much larger, it may be even beyond one monolayer. During the subsequent exposure to $SiCl_2H_2$ initially part of the $SiCl_2H_2$ is used to remove B rather then to deposit Si. The growth of Si is resumed when either growth nuclei have been formed on the B terminated surface or the B coverage decreases below one monolayer and the growth starts from Si surfaces. The data evaluated by SIMS after the deposition process are therefore the result of complex adsorption - desorption processes. Further evidence for this model is given by an experiment were the Si source was SiH_4 instead of $SiCl_2H_2$. For an B exposure time of 15s the integrated dose of B in this sample was $3x10^{15}$ cm^{-2}, more then an order of magnitude higher then for the sample where the subsequent layer was grown by $SiCl_2H_2$. This indicates that B is removed during the exposure of $SiCl_2H_2$ and that the Cl plays an imported role in the removal. The assumption of B desorption during the initial exposure to $SiCl_2H_2$ also explains the super-linear increase of the B-dose with the exposure time.

However, since no self limitation has been found, these experiments indicate that B_2H_6 is not a suitable source for a self limiting atomic layer doping process in Si by APCVD at temperatures between 400 and 600°C.

4) AsH_3 doping in APCVD

In CVD processes AsH_3 is the typical As dopant source due to the low diffusion coefficient. ALD experiments were performed in the same fashion as for the B_2H_6. Fig. 8 shows the SIMS data for three samples. Each sample was prepared

using 5 cycles with 1,2,4,8 and 16 s exposure time of the Cl/H terminated Si surface. The temperatures, T_{ALD}, of the exposures were 600, 500 and 400°C. At 400°C no As was detected by SIMS. Gravimetric techniques established that a 160 nm thick film was grown. Therefore we conclude that no As was incorporated, probably the AsH_3 is not chemisorbed at 400°C on the Cl and H terminated Si surface. Possibly physisorbed AsH_3 on the surface apparantly desorbs during the heating to the deposition temperature of 650°C before it reacts with the surface. At 500°C no AsH_3 is incorporated for short exposure times whereas the SIMS indicate some incorporation for long exposure times (8 and 16 s). For an increase of T_{ALD} to 600°C all 5 As doping spikes are clearly seen in the SIMS. The fact that incorporation occurs must be explained by changes either of the chemical termination of the surface or of the As species arriving at the surface. Cl is released from the surface via SiCl at temperatures above 700°C /2/. Time-of-flight measurements made in-situ during chemical beam epitaxy indicate that H_2 desorbs from the surface at temperatures as low as 550°C /13/, however, the situation at one atmosphere of H_2 in the APCVD reactor is unclear. It is reasonable to assume that the AsH_3 competes with a equilibrium reaction between desorption and adsorption of hydrogen, which might allow AsH_3 to chemisorb on surface sites. In addition, AsH_3 starts to decompose at these temperatures. In-situ measurements of the decomposition of AsH_3 show that the first step is surface catalysed and heterogeneous /14/. Clean quartz walls lead to decomposition temperatures as low as 600°C and wall depositions may even lower that temperature.

At 600°C the amount of As in the spikes approaches saturation at a level of $8*10^{13}$ cm^{-2} for exposure times longer then 8s. The low level of the saturation at 0.1 ML is unexpected. It might be correlated to the ratio of the parts of the Si surface terminated with H and with Cl after the growth from $SiCl_2H_2$ Further experiments using different temperatures for thc Si deposition prior and after the

AsH_3 exposure as well as detailed investigations of the surface chemistry during APCVD from $SiCl_2H_2$ might help to clarify this observation.

General factors contribute to the rather poorly resolved (low peak to valley ratio) of the As dopant spikes we have observed. Unfortunately, as in the case of Sb in the MBE experiments, the As tends to segregate leading to a smearing of the As into the subsequently grown Si. In addition a rather long residence time for As is observed in our tool. The in-situ incorporation of As from AsH_3 into the Si leads to growth rate enhancement of Si from $SiCl_2H_2$ /15/ which accounts for the increase of the thickness of the Si layer inbetween the As spikes. However, the observation of a self-limiting process for As doping has some promise for atomic layer doping in CVD techniques to meter precise As doses into Si.

D) Conclusion

We have investigated different methods to incorporate atomic layer doping both in MBE and CVD enviroments. So far we have determined that Self Limiting reactions do occur for n-type dopants Sb and AsH_3. However, these species also have the problem of surface segregation. B_2H_6 was not found to self limit in the process parameter space explored in the experiments we have described, though at low temperatures, it is expected to self limit. In addition the experiments permit a new way of looking into surface kinetics for doping in APCVD and GSMBE which may impact the optimization of growth in the future.

E) Acknoledgements

We would like to acknoledge the support from J. Cotte and F. Cardone supplying the SIMS data. One of us (SSI) would like to thank R.A. Metzger (Hughes Research, Malibu) for useful discussions.

Figure captions

Fig.1: Schematic of ALD process

Fig.2: APCVD temperature and gasflow sequence for ALD using the exposure time, t_p, and the temperature at time of dopant exposure, T_{ALD}, as parameter

Fig.3: Sb on Si (100) Desorption Spectra and surface reconstructions (from R.A. Metzger, Ph.D. Dissertation, 1983)

Fig.4: SIMS profile of a Boron spike deposited at 550°C from B_2H_6 by MBE

Fig.5: Dependence of the B sheet density determined by SIMS on the B_2H_6 exposure for MBE grown samples

Fig.6: Dependence of the B sheet density determined by SIMS on the B_2H_6 exposure time for APCVD grown samples

Fig.7: Effect of the Boron surface concentration on the thickness of the subsequent grown Si cap layer

Fig.8: SIMS profiles of 3 Si samples exposed to AsH_3 during growth interruptions at 400, 500 and 600°C with exposures times of 1, 2, 4, 8 and 16 s for each sample

References

/1/ J. Nishizawa, K. Aoki, S. Suzuki and K. Kikuchi
J. Cryst. Growth 99, 502 (1990)

/2/ J.A. Yarmoff, D.K. Shuh, T.D. Durbin, C.W. Lo, D.A. Lapiano-Smith
F.R. McFeely and F.J. Himpsel
presented at the American Vacuum Society, Seattle, Washington
Nov. 10-15 (1991)

/3/ A.R. Powell, R.A.A. Kubiak, E.H.C. Parker, D.K. Bowen, and
M. Polcarova
Proc. Mat. Res. Soc. 206, 161 (1991)

/4/ D.A. Grützmacher and T.O. Sedgwick
to be published

/5/ D.J. Gravesteijn, P.C. Zalm, G.F.A van de Walle, C.J. Vriezma,
A.A. van Gorkum, L.J. Ijzendoorn
Thin Solid Films 183, 191 (1989)

/6/ D.A. Grützmacher, A.R. Powell, T.O. Sedgwick, S.S. Iyer, and J. Cotte
to be published

/7/ D. Grützmcher, J. Hergeth, F. Reinhardt, K. Wolter, and P. Balk
J. Electron. Mater. 19, 471 (1990)

/8/ R.A. Metzger, Ph.D. Dissertation (1983)

/9/ F.K. LeGoues, V.P. Kesan, S.S. Iyer, J. Tersoff, R. Tromp
Phys. Rev. Lett. 64, 2038 (1990)

/10/ S.J. Fukatsu, S. Kubo, Y. Shiraki, R. Ho
J. Cryst. Growth 111, 843 (1991)

/11/ L.J. van Ijzendoorn, C.W. Fredriksz, C. van Opdrop, D.J. Gravesatejn, D.E.W. Vandenhoudt, G.F.A. van de Walle, C.W.T. Bulle Lieuwma
Ion Beam Analysis: 10th Intern. Conf., Eindhoven, Netherlands 1-5 July 1991, Nucl. Instrum. Methods Phys. Res. B 64, 120 (1992)

/12/ Ming L. Yu, D.J. Vitkavage, B.S. Meyerson
J. Appl. Phys. 59, 4032 (1986)

/13/ S.M. Gates, S.K. Kulkarni
Appl. Phys. Lett. 60, 53 (1992)

/14/ W. Richter, P. Kurpas, R. Lückerath, M. Motzkus, and M. Waschbüsch
J. Cryst. Growth 107, 13 (1991)

/15/ P. Agnello, T.O. Sedgwick, M.S. Goorsky, J. Cotte
Appl. Phys. Lett. 60, 454 (1992)

Sticking coefficient S : for diff. B densities

10^{9} cm^{-2} – S=2.7x10^{-3}
10^{11} cm^{-2} – S=1.7x10^{-3}
10^{12} cm^{-2} – S=1.5x10^{-3}
10^{14} cm^{-2} – S=0.3x10^{-3}

Tab I

Atomic Layer Doping

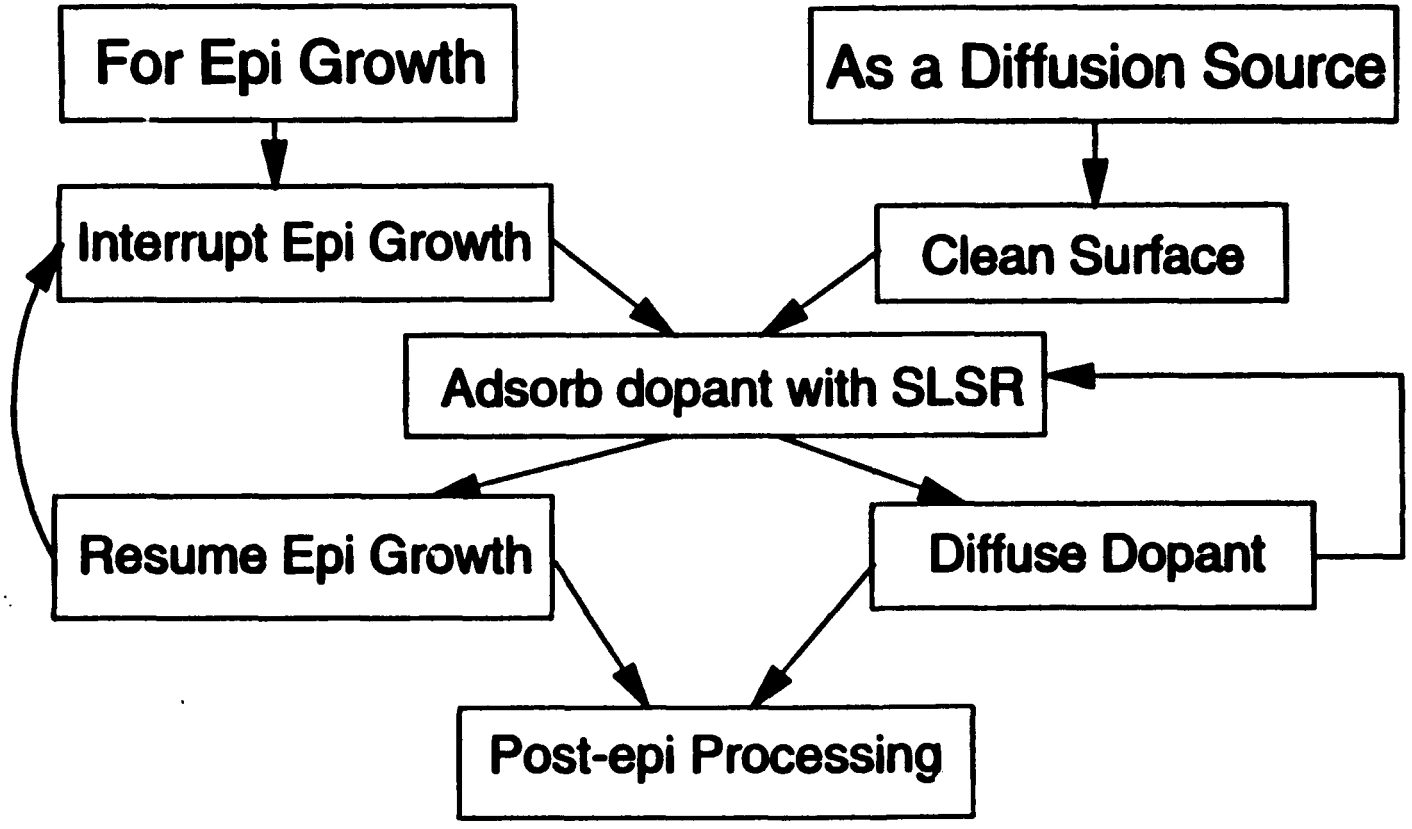

Fig 1

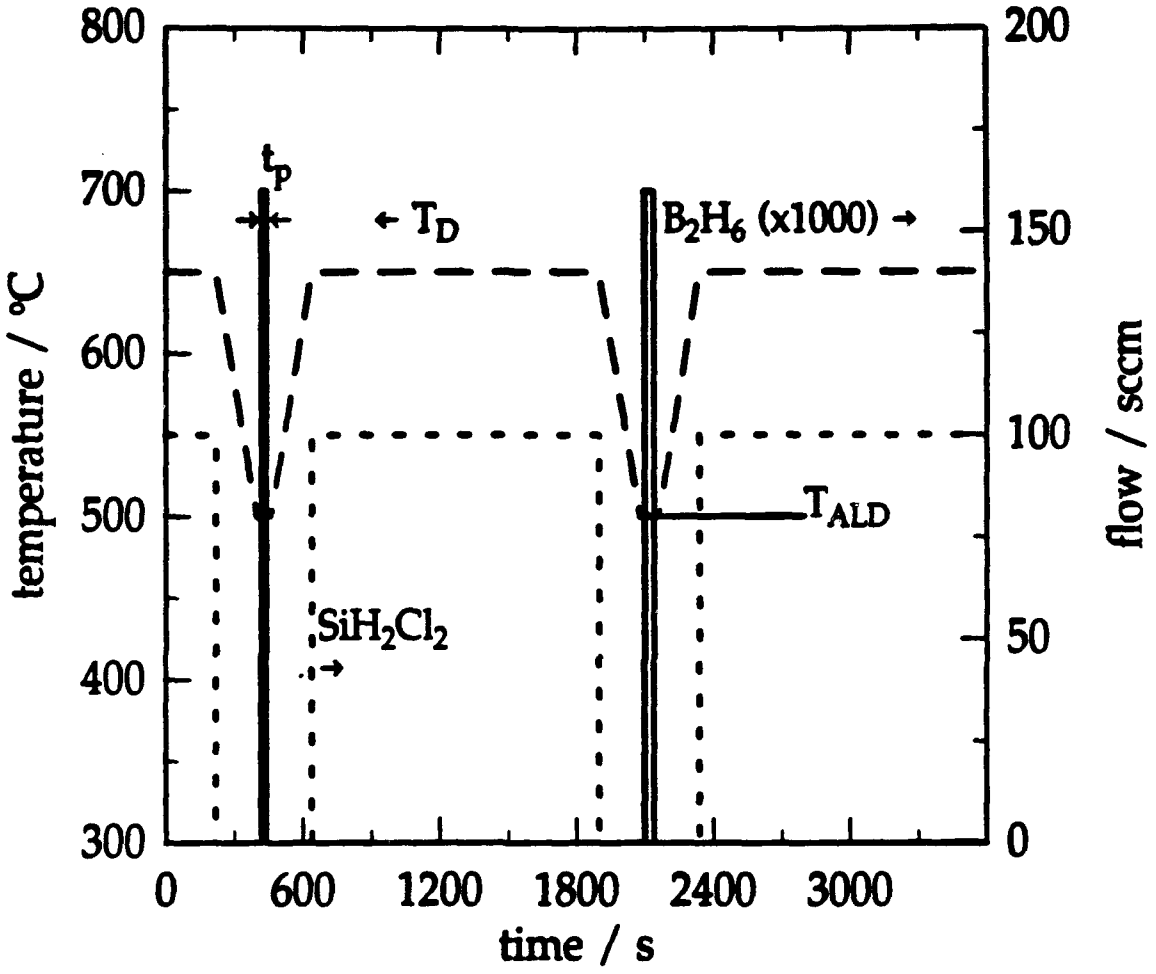
800
700
600
500
400
300
200
150
100
50
0
temperature / °C
flow / sccm
t_P
← T_D
B_2H_6 (x1000) →
T_{ALD}
SiH_2Cl_2 →
0
600
1200
1800
2400
3000
time / s

Fig 2

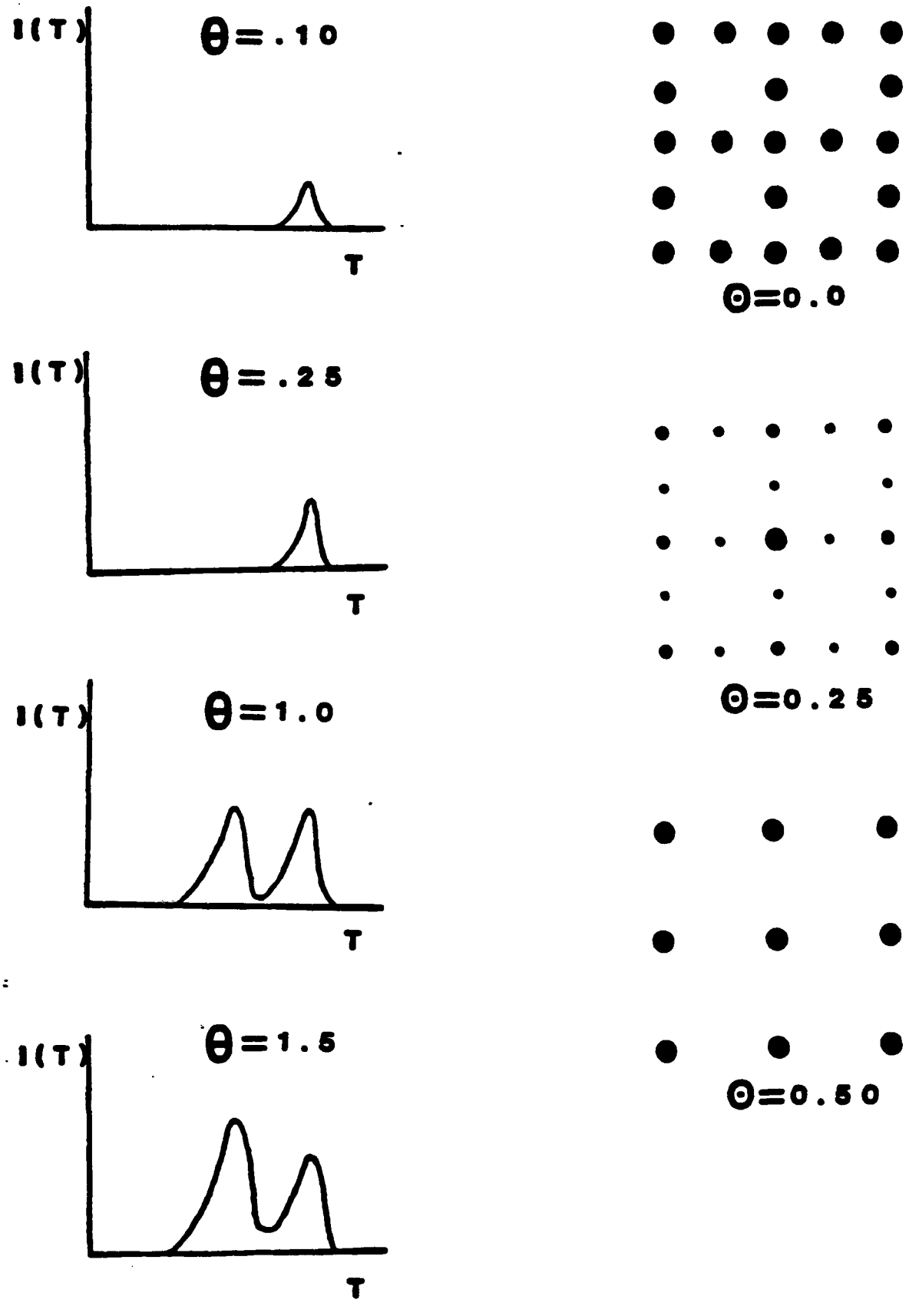

Fig 3

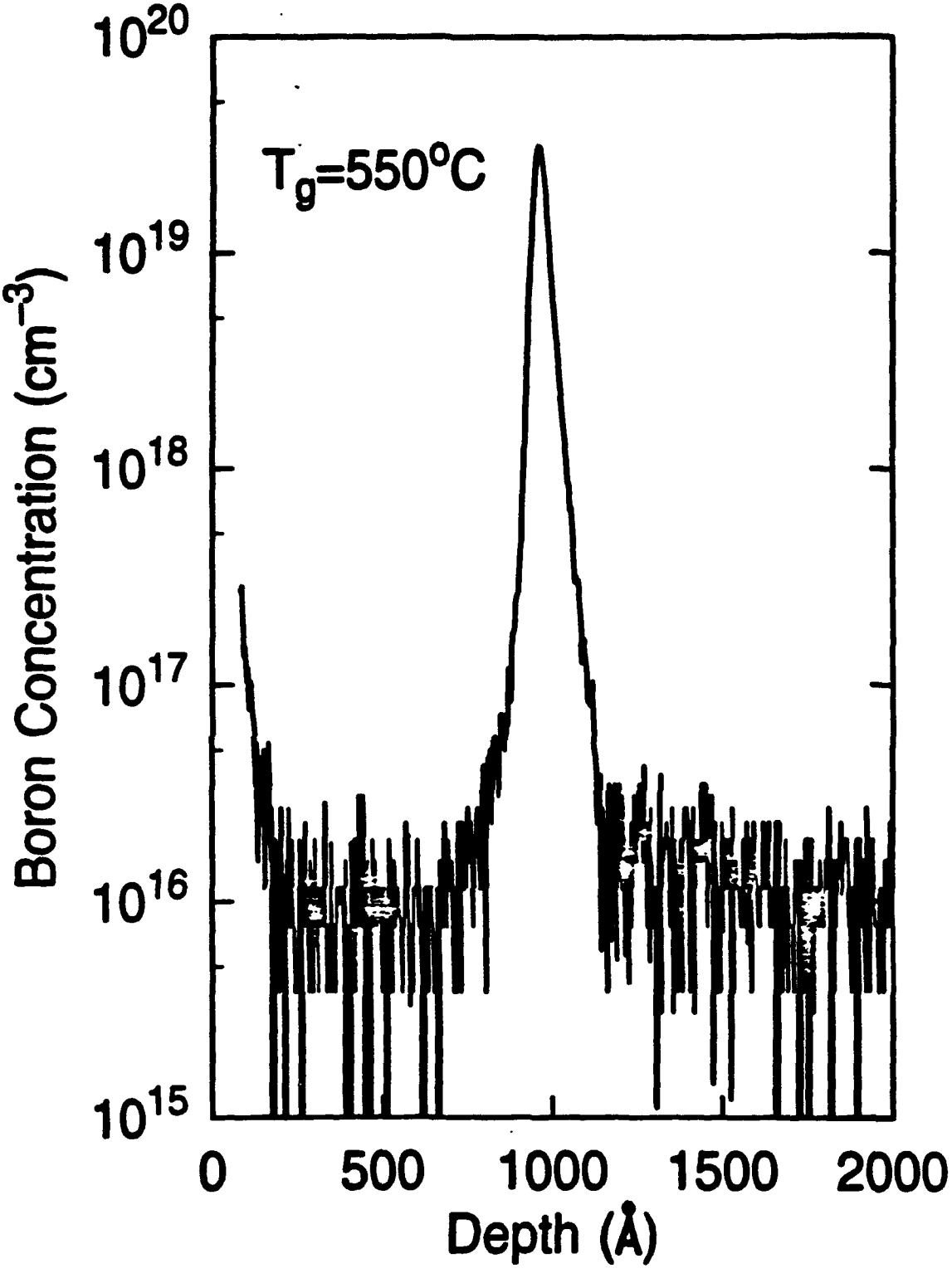
10^{20}
10^{19}
10^{18}
10^{17}
10^{16}
10^{15}
T_g=550°C
Boron Concentration (cm^{-3})
0
500
1000
1500
2000
Depth (Å)

Fig 4

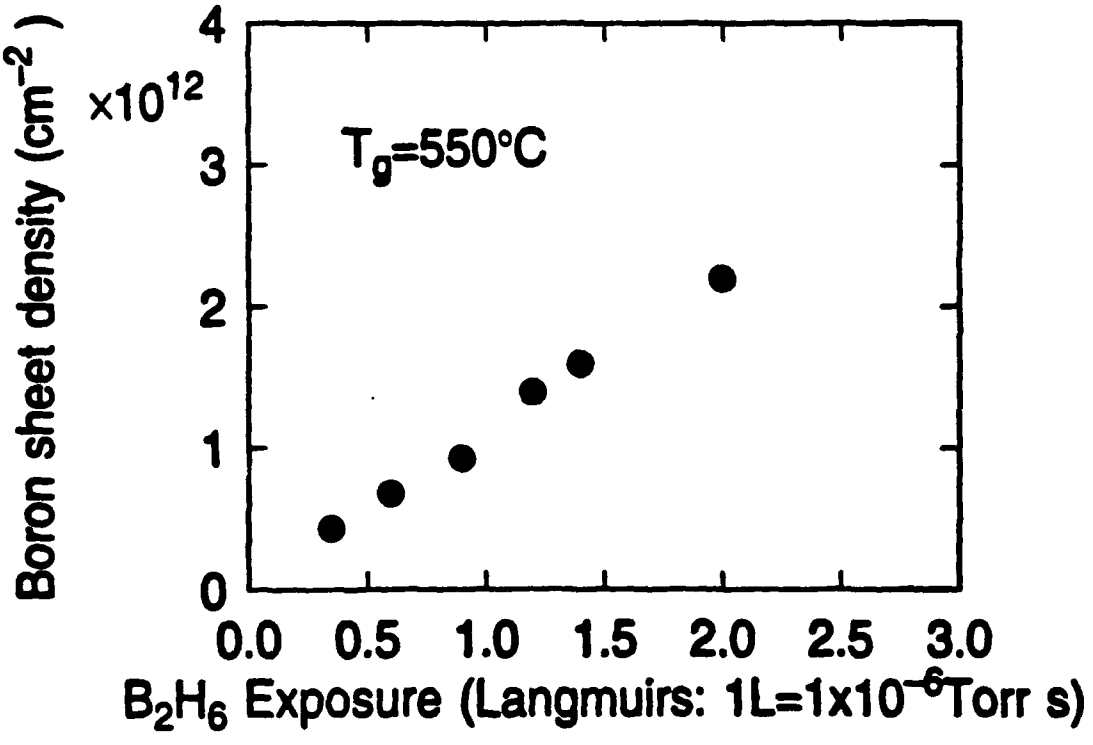
Boron sheet density (cm^{-2})
$\times 10^{12}$
4
3
2
1
0
T_g=550°C
0.0
0.5
1.0
1.5
2.0
2.5
3.0
B_2H_6 Exposure (Langmuirs: 1L=1x10^{-6}Torr s)

Fig 5

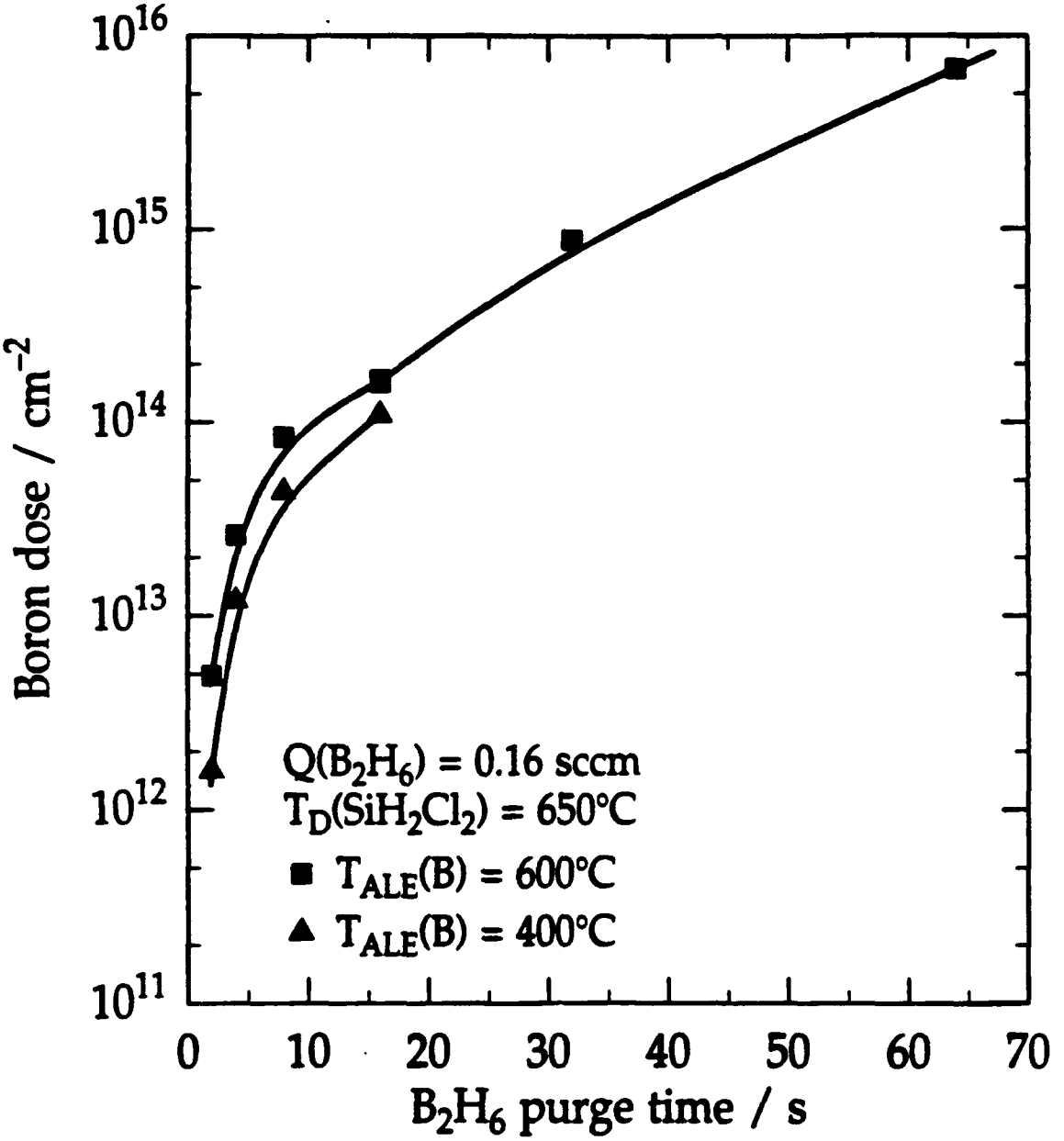
Boron dose / cm^{-2}
10^{16}
10^{15}
10^{14}
10^{13}
10^{12}
10^{11}
$Q(B_2H_6)$ = 0.16 sccm
$T_D(SiH_2Cl_2)$ = 650°C
$T_{ALE}(B)$ = 600°C
$T_{ALE}(B)$ = 400°C
0
10
20
30
40
50
60
70
B_2H_6 purge time / s

Fig 6

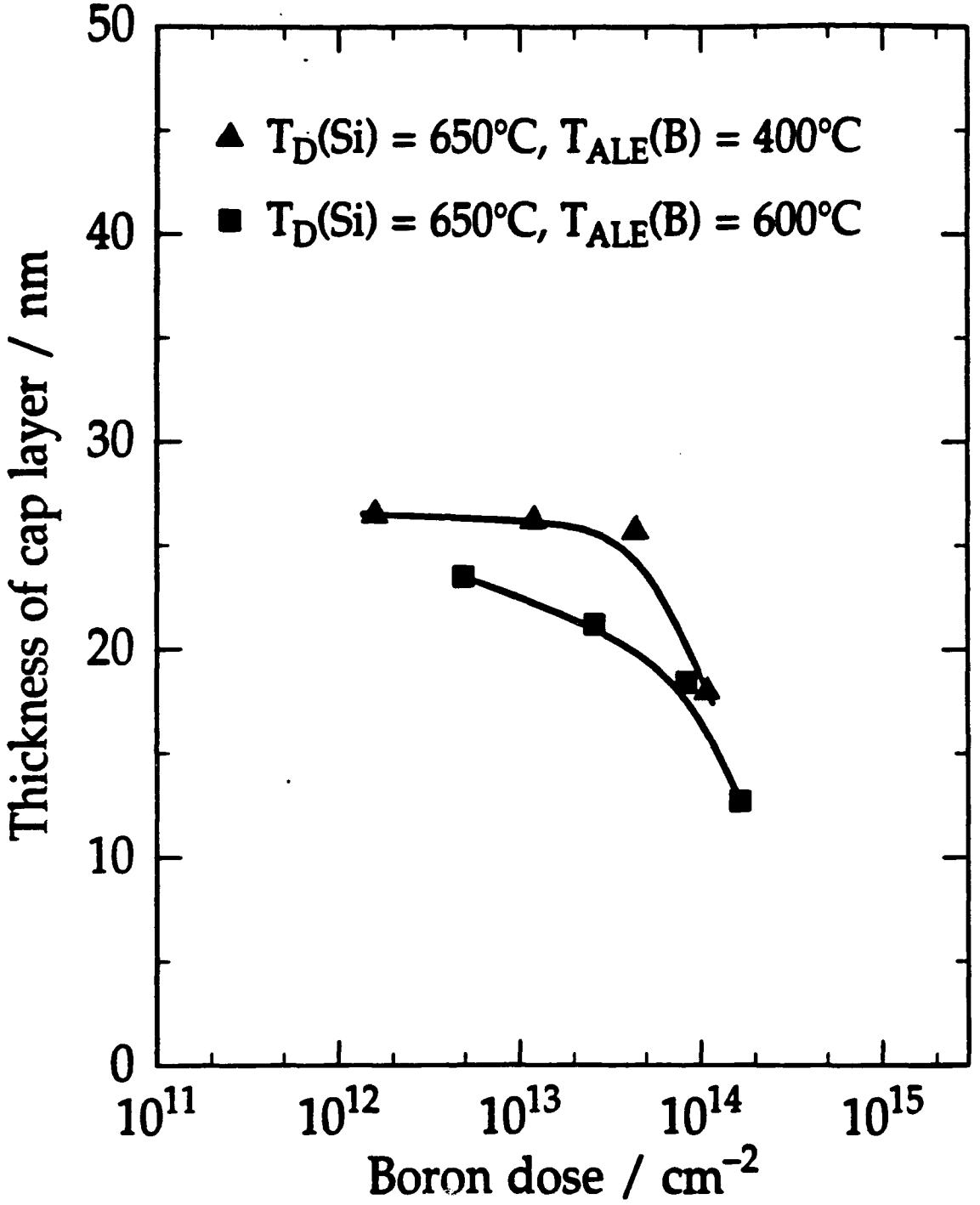
50
40
30
20
10
0
▲ T_D(Si) = 650°C, T_{ALE}(B) = 400°C
■ T_D(Si) = 650°C, T_{ALE}(B) = 600°C
Thickness of cap layer / nm
10^{11}
10^{12}
10^{13}
10^{14}
10^{15}
Boron dose / cm^{-2}

Fig 7

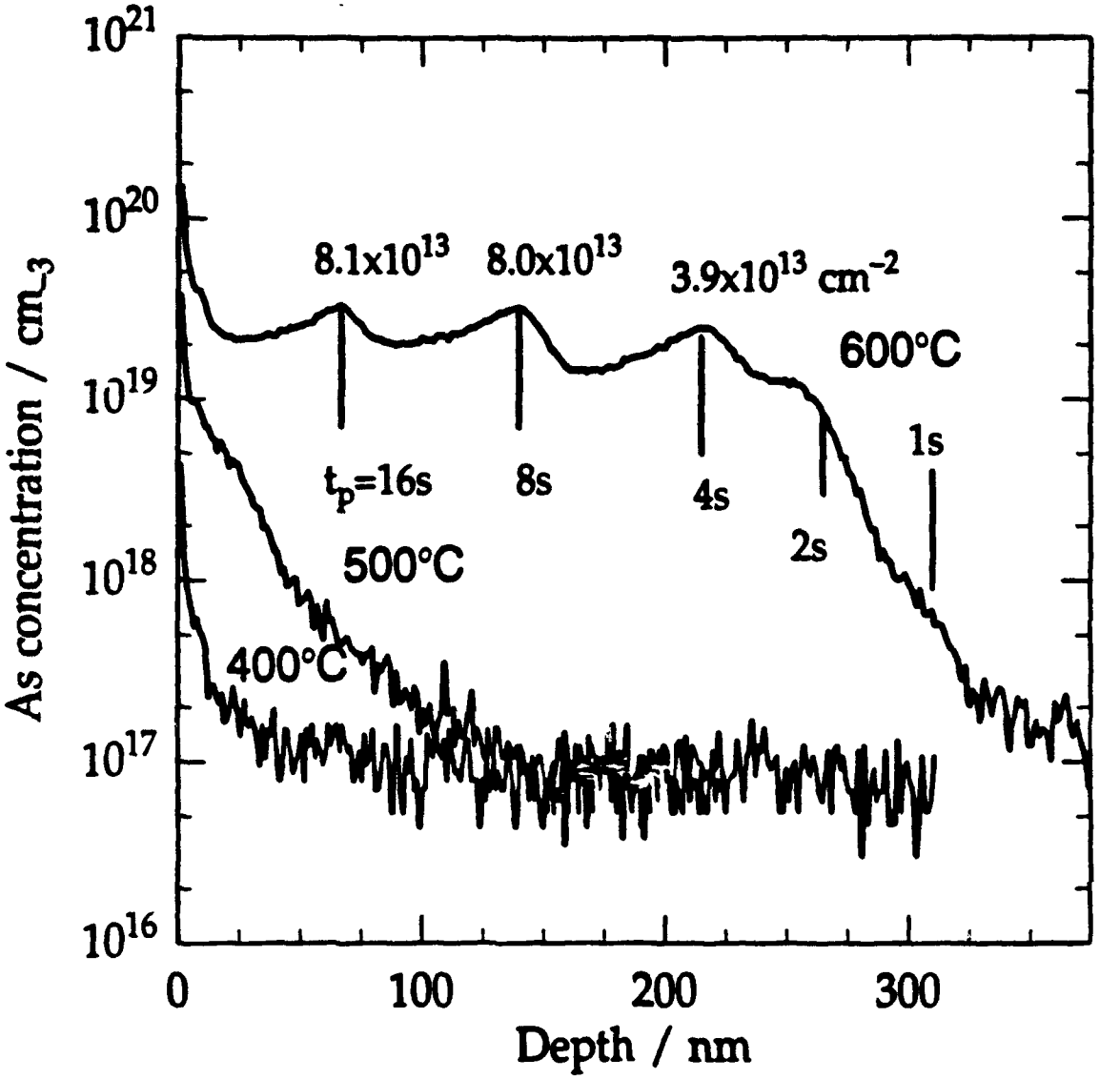
10^{21}
10^{20}
10^{19}
10^{18}
10^{17}
10^{16}
As concentration / cm_{-3}
8.1x10^{13}
8.0x10^{13}
3.9x10^{13} cm^{-2}
600°C
t_p=16s
8s
4s
2s
1s
500°C
400°C
0
100
200
300
Depth / nm

Fig 8

Appendix D

Silicon-Germanium-Carbon Alloys Extending Si Based Heterostructure Engineering

1 Introduction

This area of research is aimed at producing random alloys of low C composition $Si_{1-y}C_y$ and $Si_{1-x-y}Ge_x C_y$ alloys. The growth of these alloys should offer new possibilities in band engineering on Si substrates. There are possibilities for high electron mobility FET devices grown pseudomorphicaly on Si. In addition we are examining the band structure of these alloys, with the hope of producing a material with higher transmission probability for optical emission than Si, from either high Ge content $Si_{1-x-y}Ge_x C_y$ alloys or zone folded superlattices, both of which can be grown pseudomorphically on Si (100). Much of our preliminary work has been carried out using solid sources. As the use of solid sources, for the matrix fluxes, can not provide atomic layer epitaxy we are now investigating the production of these alloys of Ge, C and Si with gas sources where ALE may be achieved. In the previous six months we have been concentrating on incorperating gas sources into the MBE system. We now have the ability to flow four different gas types into the system thus we can grow with a) solid sources, b)mixed solid and gas sources, and c) only gas sources. We are presently investigating the incorporation properties of acetylene gas. We are examining this both in the low temperature range where low composition $Si_{1-y}C_y$ alloys are formed, and in the high temperature range where silicon carbide is created, in this section we shall discuss the former of these two regimes.

In the past ten years epitaxial SiGe material has proved itself to be of high crystalline quality and has provided impressive results in bandgap engineered device structures .. [1,2] The addition of Ge onto the Si lattice provides compressive strain, this reduces the bandgap by splitting the six fold degeneracy of the conduction band and lowering the 4 fold degenerate conduction valley Δ_4 [4]. However there are limits imposed within the system, and tensile stress is not available without the use of thick buffer layers[4,5,6] which have, at best a threading dislocation density of $10^4\ cm^{-2}$ for x = 0.3 buffers. When C is added to Si, the grown layer is under tensile strain, this again splits the degeneracy and this time the 2 fold degenerate conduction band Δ_2 is expected to be lowered, thus giving a net reduction in the bandgap for strained $Si_{1-y}C_y$ material. In addition the Δ_2 conduction valley has light in plane electron mass and therefore should provide high mobility devices.

For cubic, i.e. relaxed $Si_{1-y}C_y$ material, where there is no strain induced shrinkage of the bandgap, the bandgap should increase towards the value of 2.2eV for the 50% alloy, β-SiC. As the band structures of Si and β-SiC are quantitatively similar, with the conduction band minima positioned near the X(100) zone edge there should be no question of an L-X crossover[7], as in the SiGe case.

2 Growth of $Si_{1-y}C_y$ alloy

Growth of the $Si_{1-y}C_y$ random alloy is more limited than the SiGe case as the C is not miscible with Si, it has a solubility of $< 10^{-6}$ at 1400°C. At higher temperatures the more stable carbide phases are formed however if the growth temperature is reduced such that the growth can be kinetically stabilized then the random alloy may be deposited. The second important aspect of $Si_{1-y}C_y$ is that the lattice mismatch to Si is high 52% (for diamond). However, as in this work it is the induced strain that is important, only low compositions of $Si_{1-y}C_y$ alloy are required. For example, 1% of C gives approximately the same magnitude of strain as 11% of Ge in the Si matrix.In the preliminary work we have used solid elemental carbon (graphite) filament which is heated to in excess of 3000°C in order to sublime C atoms from the filament. This provides a flux rate controllable from the applied current of up to 0.01 nm/sec, this is acceptable for the growth of low C composition $Si_{1-y}C_y$ alloys but would be too low for practicable growth of β SiC. Having demonstrated the ability to grow $Si_{1-y}C_y$ and $Si_{1-x-y}Ge_xC_y$ alloys with the solid C source we are now using acetylene to produce the alloys and anticipate the use of both Disilane and Germane in

the near future. The gas sources have been attached to a solid source Molecular Beam Epitaxy (MBE) system and pumping during growth is achieved using a turbomolecular pump. The base pressure of the system remains in the 10^{-10} torr regime and rises to $5x10^{-9}$ torr during the growth of the Si layers. To deposit the $Si_{1-y}C_y$ layers the acetylene is injected into the system to bring the pressure up to $2x10^{-7}$ torr. The growth temperatures for the $Si_{1-y}C_y$ deposition are between 500°C and 600°C. The acetylene provides an over- pressure of gas and therefore the composition of the $Si_{1-y}C_y$ layer is controlled by the Si flux rate, typically 1 to 10 nm/min. The high epitaxial quality of the $Si_{1-y}C_y$ grown with the solid C source has been previously demonstrated[9]. The Gas Source Molecular Beam Epitaxy (GSMBE) also gives high quality epitaxial material, Fig 1 shows the the X-ray diffraction (004) rocking curves obtained for two samples grown utilizing the acetylene gas source. The solid curve is for a 100nm $y = 0.015$ $Si_{1-y}C_y$ layer grown to close to the metastable critical thickness for this temperature (140nm). The same composition layer grown at the higher temperature of 600°C was indeed found to be relaxed. The presence of the pendellosung peaks in the rocking curves shows that the material is of good crystalline quality, as dislocations in the material produce localized strain fields which wash out the pendellosung fringes. The quality of the $Si_{1-y}C_y$ grown utilizing the gas source can be seen from the lack of any additional broadening of the X-ray diffraction rocking curve.

3 $Si_{1-x-y}Ge_xC_y$ Material

The critical thickness values for $Si_{1-y}C_y$ alloy are found to be significantly more stringent than for the $Si_{1-x}Ge_x$ alloy[8] (at 500 o.C the metastable critical thickness of $Si_{1-y}C_y$ is approximately ten times less than that of $Si_{1-x}Ge_x$ grown on Si). One approach to overcome this limitation is to consider the ternary alloy $Si_{1-x-y}Ge_xC_y$ where the compressive strain induced by the Ge atoms can be countered for by the tensile strain caused by the addition of C atoms to the matrix. By combining Ge and C in the correct ratio, 1:11, an alloy can be produced that is lattice matched to Si and therefore has no critical thickness limitation.

We have used both the solid and gas sources to produce $Si_{1-x-y}Ge_xC_y$ material, (the latter in this case), in Fig 1 we show a $Si_{1-y}C_y$ layer (solid line), and (dashed line) a sample grown under the same growth conditions except that 15 % of Ge has been added to equalize the strain i.e., 100nm $C = 0.015$ $Ge = 0.15$ $Si_{1-x-y}Ge_xC_y$. The pendellosung peaks are still clearly seen for the strain equalized sample, indicating high quality crystal, and the net mismatch of the layer is only $7x10^{-4}$.

4 Superlattice Deposition

A second method for producing a strain equalized structure on Si is to deposit alternate layers of $Si_{1-x}Ge_x$ and $Si_{1-y}C_y$ to produce a strain symmetrical structure on Si. One aim of this type of structure is to examine "zone folding" effects in a very high mismatch superlattice. If a superlattice can be produced with alternate layers of $Si_{1-y}C_y$ and Ge then the mismatch at the interface could be raised to as high as 10%, this is significantly larger than the mismatch of 4% presently under examination in the Ge, Si superlattices produced by a number of groups[11,12].

For this work we utilized the solid C source to produce short period (1.3nm) symmetrically strained superlattices. These structures consist of alternating $Si_{1-y}C_y$ and SiGe layers. The structures were grown at temperatures ranging from 500°C for low composition alloys to 475°C for the higher composition alloys, in addition to this Sb was deposited on the structure prior to the superlattice growth to provide sufactant action during deposition in order to prevent Ge segregation. A number of structures were grow with nominal compositions shown in table I.

Table I

Sample	$Si_{1-y}C_y$	$Si_{1-x}Ge_x$	Number Of Periods
1	0.5nm y = 0.03	0.8nm x = 0.2	140
2	0.8nm y = 0.025	0.5nm x = 0.4	140
3	0.8nm y = 0.035	0.5nm x = 0.55	140
4	0.8nm y = 0.06	0.5nm x = 1.0	83

The material quality of the superlattice structures degrades as the C and Ge compositions are increased. This is due to difficulties in producing high composition $Si_{1-y}C_y$ alloys without the introduction of SiC precipitates. However even at compositions as high as 55% Ge we are still able to produce sufficiently high quality material to give clear rocking curves in x-ray diffraction.

Fig 2 shows the (004) double crystal rocking curve for sample no 3. This curve clearly shows the "-1" superlattice peak at -15500 arcsec, from the superlattice peak separation the average period can be accurately found to be 1.30 nm with an error of 0.02nm. In addition near the "-1" peak it can be seen that some of the diffracted signal has been shifted into the nearby pendellosung peaks, this is due to some small period dispersion within the superlattice structure[10]. The "0" order superlattice peak at - 450 arcsec shows that there is a small amount, $1.9x10^{-3}$, of unequallized strain remaining in the superlattice. However, this is considerably less than the expected $9.2x10^{-3}$ that would be seen without the presence of the C.

For zone folding to be successful the interface quality between layers must be abrupt so as to introduce a new crystal periodicity to the lattice. It is here that an ALE process would provide a great advantage. However,even if a self limiting process is not found we hope that the installed gas sources will allow an improvement in the overall quality of the high composition alloys. In order to determine the interface quality within the superlattice structure X-ray reflectivity was used which is sensitive to both short range and long range roughness in the interfaces[13]. Fig 3 shows the curve obtained from sample #3 along with three simulations demonstrating how the intensity in the reflectivity peak decreases with increasing interface roughness.

In the reflectivity curve intensity, has again been transferred into subsidiary pendellosung peaks from the main superlattice peak. However, in this measurement it is the total integrated intensity around the superlattice peak which is important. We find that this integrated intensity is such that it can be matched by simulations with interface roughness values lower than 0.3 nm. At roughness greater than this the peak intensity is seen to rapidly fall off. At roughness values of less than 0.25 nm the interface roughness can be dominated by the random nature of the $Si_{1-x}Ge_x$ and $Si_{1-y}C_y$ alloys and thus roughness values less than this can only be considered meaningful for superlattices consisting of elemental layers such as a Si, Ge superlattice.

For sample #4 the (004)X-ray diffraction showed a small "-1" peak in a similar position to that found in Fig 2 however the peak intensity was only 1/20 of that for sample #3. From this we are able to deduce that only part of the $Si_{1-y}C_y$, Ge superlattice was deposited in a crystalline form. However, the diffraction data is able to determine that the structures period is indeed 1.35 nm, and the peak intensity suggests that five to ten periods of superlattice were deposited before the material lost crystal quality. Transmission Electron Microscopy (TEM) of the $Si_{1-y}C_y$, Ge superlattice, as can be seen the structure is initially deposited commensurate with the underlaying Si however after approximately seven periods there is a transition to amorphous growth. We have here demonstrated that it is possible to deposit $Si_{1-y}C_y$, Ge short period superlattices. These are lattice matched to Si, and the mismatch at each interface of the superlattice is 7%, considerably larger than the interface mismatch obtained for Si, Ge superlattices deposited on $Si_{1-x}Ge_x$ where x = 0.5.

5 Conclusions

In this work we have demonstrated high quality growth of $Si_{1-y}C_y$ and $Si_{1-x-y}Ge_xC_y$ material using both solid, and gas, sources for the C flux. Two differing methods for overcoming the strain limitations inherent in the $Si_{1-x}Ge_x$ and $Si_{1-y}C_y$ alloy systems have been demonstrated.

The first approach of creating a ternary alloy produces high quality material with no strain present except on a very localized scale. The band structure of high Ge and C composition $Si_{1-x-y}Ge_x C_y$ material has yet to be examined and it may offer interesting possibilities, if it is found to be qualitatively similar to Ge it could have significant potential.

The second alternative for equalizing the strain uses the opposing strains of the $Si_{1-x}Ge_x$ and $Si_{1-y}C_y$ alloy layers to eliminate the net strain. This may offer new opportunities in device engineering or alternatively a new approach to the idea of Brillouin zone folding may yield a quasi-direct bandgap material which can be deposited on Si. We have demonstrated that short period superlattices can be deposited on Si with a high degree of control of the period, and the interface roughness both in terms of short and long range disorder.

References

1. G.L.Patton, J.M.Stork, B.S.Myerson, and D.L.Harame: IEEE Electron Dev. Lett. 11 .171, (1990)
2. V.P.Kesan, P.G.May, G.V.Treyz, E.Bassous, S.S.Iyer, and J.M.Halbout: Mat Res Soc Symp. Proc. 220, 471
3. R.People: IEEE J.Quantum Electron. QE-22 1696 (1986)
4. A.R.Powell, R.A.Kubiak, T.E.Whall, E.H.C.Parker, and D.K.Bowen: Mat Res Soc Symp. Proc. 220, 277
5. E.A.Fitzgerald, Y.H.Xie, M.L.Green, D.Brasen, A.R.Kortan, Y.J.Mii, J.Michel, B.E.Weir, L.C.Feldman, and J.M.Kuo: Mat Res Soc Symp. Proc. 220, 211
6. F.K.LeGoues, B.S.Myerson, J.F.Morar, P.D.Kirchner: J.Appl. Phys. 71 4230 (1929)
7. R.A.Soief: J.Appl. Phys. 70 (1991) 2740.
8. A.R.Powell, K.Eberl, B,A.Ek, and S.S.Iyer: J.Cryst Growth 127 (1993) 425.
9. A.R.Powell, K.Eberl, F.K.LeGoues, B,A.Ek, and S.S.Iyer: J.Vac. Sci. Technol. B 11 (1993) 1064
10. A.R.Powell, R.A.A.Kubiak, D.K.Bowen, and M.Polcarova: Proc. Mat. Res. Soc 208 (1991) 113.
11. T.P.Persall, J.M.Vandenberg, R.Hull, and J.M.Bonar: Phys. Rev.Lett 63 (1989) 2104.
12. S.C.Jain, and W.Hayes: Semicond. Sci. Technol. 6 (1991) 547
13. A.R.Powell, D.K.Bowen, M.Wormington, R.A.A.Kubiak, E.H.C.Parker, J.Hudson, and P.Augustus: Semicond. Sci. Technol. 7 (1992) 627

Fig 1 Experimental and simulation X-ray diffraction, (004), of a 100nm y = 1.5% $Si_{1-y}C_y$ layer(solid line) and form a 100nm y = 1.5% x = 15% *Si* layer. Both show clear pendellosung peaks indicative of good crystal quality.

Fig 2 Experimental and simulation X-ray diffraction rocking curves, (004), of sample #3, a short period superlattice with $Si_{1-y}C_y$ and $Si_{1-x}Ge_x$ layers. The "0" order superlattice peak can be seen just to the left of the substrate peak and the "-1" peak can be seen at -15000 arcsec.

Fig 3 Experimental and simulation reflectivity curves of sample #3 showing the first superlattice reflectivity peak, at 12000 arcsec. In this much of the intensity from the first order peak has been transferred into the adjacent pendellosung peaks.

Fig 1

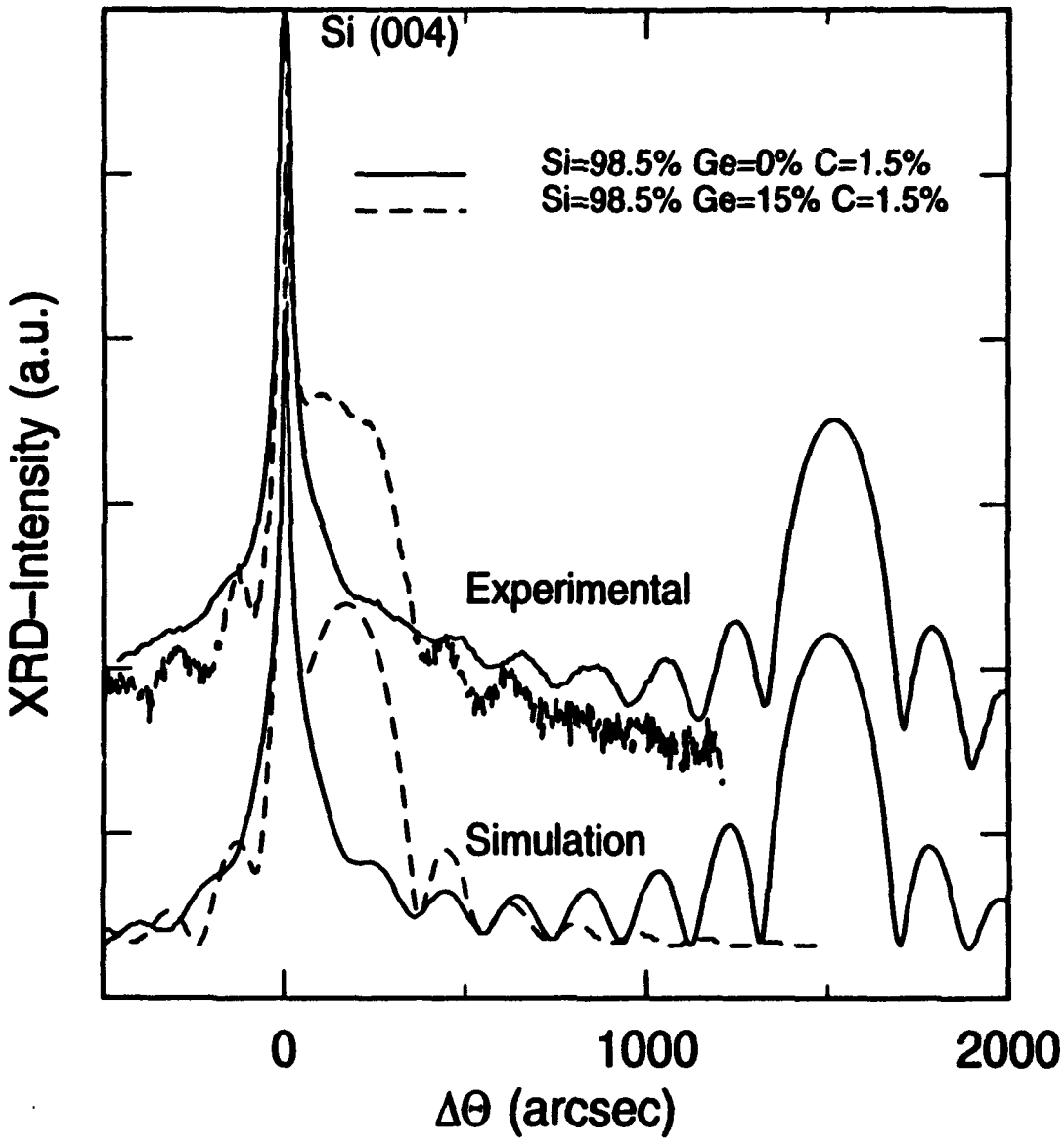
Si (004)
Si=98.5% Ge=0% C=1.5%
Si=98.5% Ge=15% C=1.5%
Experimental
Simulation
XRD–Intensity (a.u.)
0
1000
2000
Δθ (arcsec)

Fig 2.

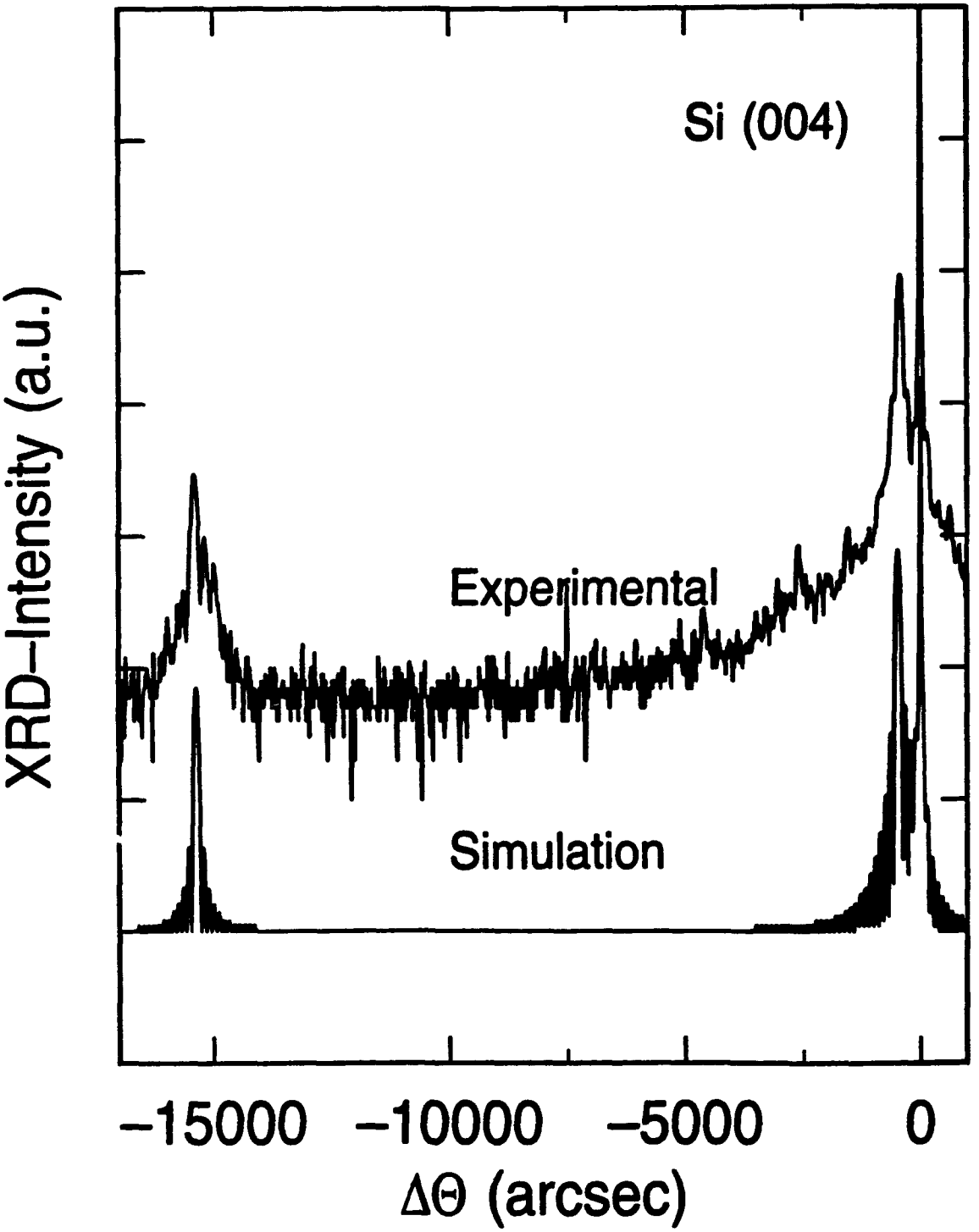
Si (004)
Experimental
Simulation
XRD–Intensity (a.u.)
–15000
–10000
–5000
0
ΔΘ (arcsec)

Fig 3

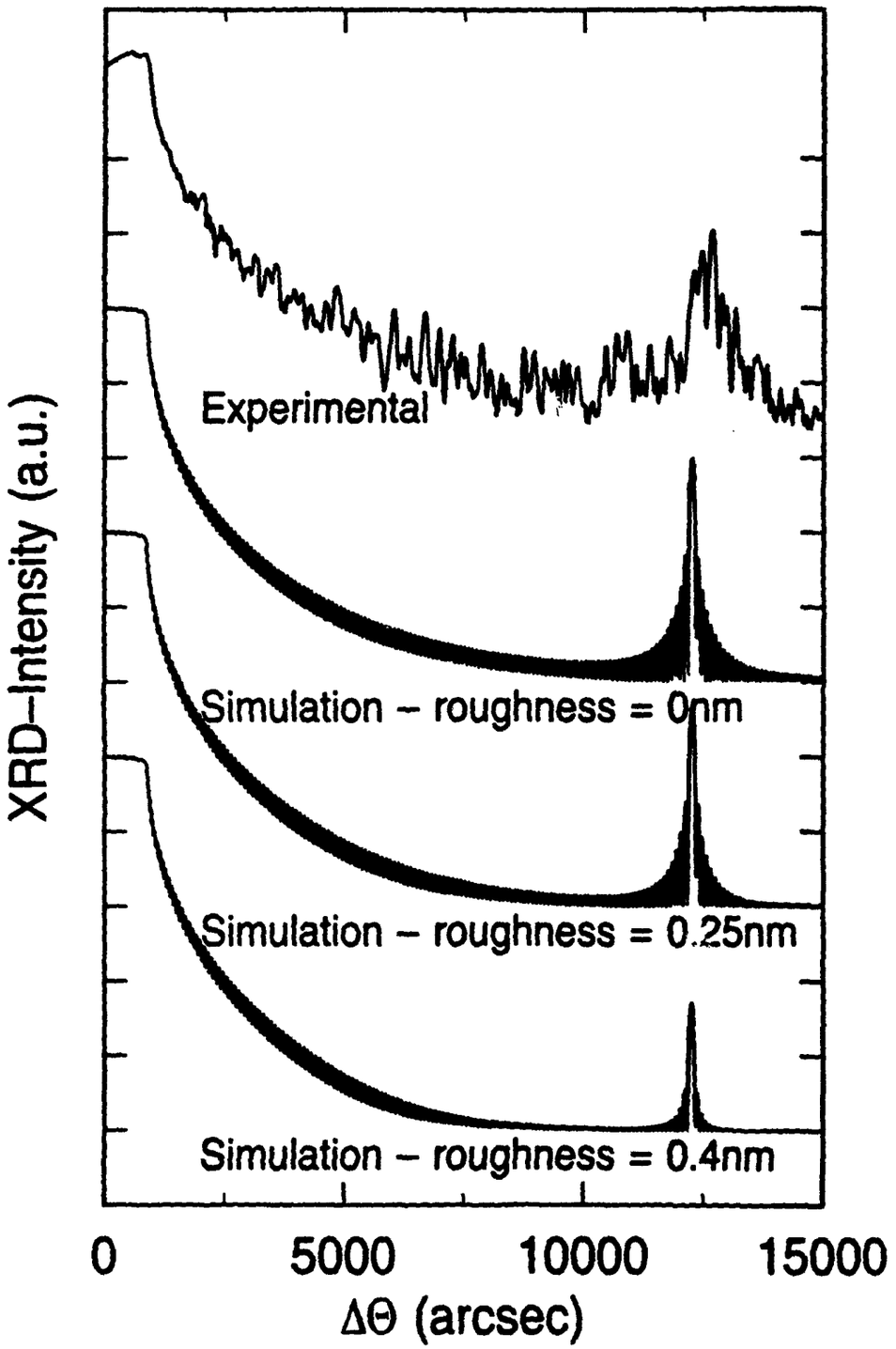
XRD–Intensity (a.u.)
Experimental
Simulation – roughness = 0nm
Simulation – roughness = 0.25nm
Simulation – roughness = 0.4nm
0
5000
10000
15000
ΔΘ (arcsec)